
Polar aurora: from the solar wind
to light emissions.
Space weather.
Seminaire LPSC 05/06/2014

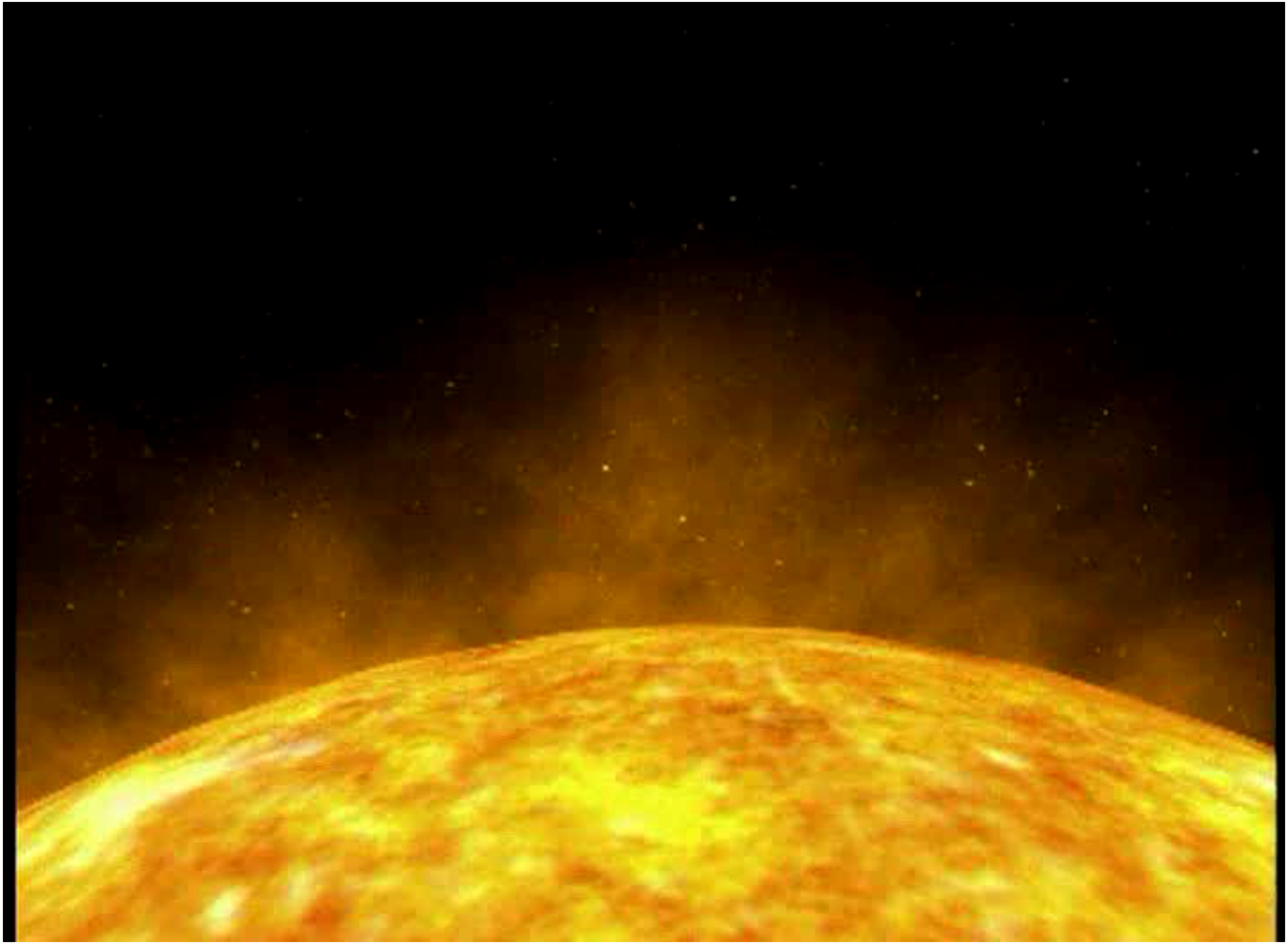

Il existe trois sources majeures (sources pour la Terre, pertes pour l'étoile) d'énergie issue du Soleil qui vont présider à la formation de l'ionosphère et de la magnétosphère terrestres. Leurs caractéristiques principales sont :

	Caractère	*Energie*	*Effet sensible sur Terre après*
Vent solaire (lent et rapide)	Permanent	10^4 W.m^{-2}	*3* jours
Spectre UV	Permanent	10^5 W.m^{-2}	*8* minutes
Eruptions	Sporadique	10^6 W.m^{-2}	*2* à *3* jours

Le vent solaire possède, au niveau de la Terre, une vitesse variable de *200* à *800* km.s^{-1} et une densité d'environ *5* particules par mètre cube. Son champ magnétique moyen est *8* nT.

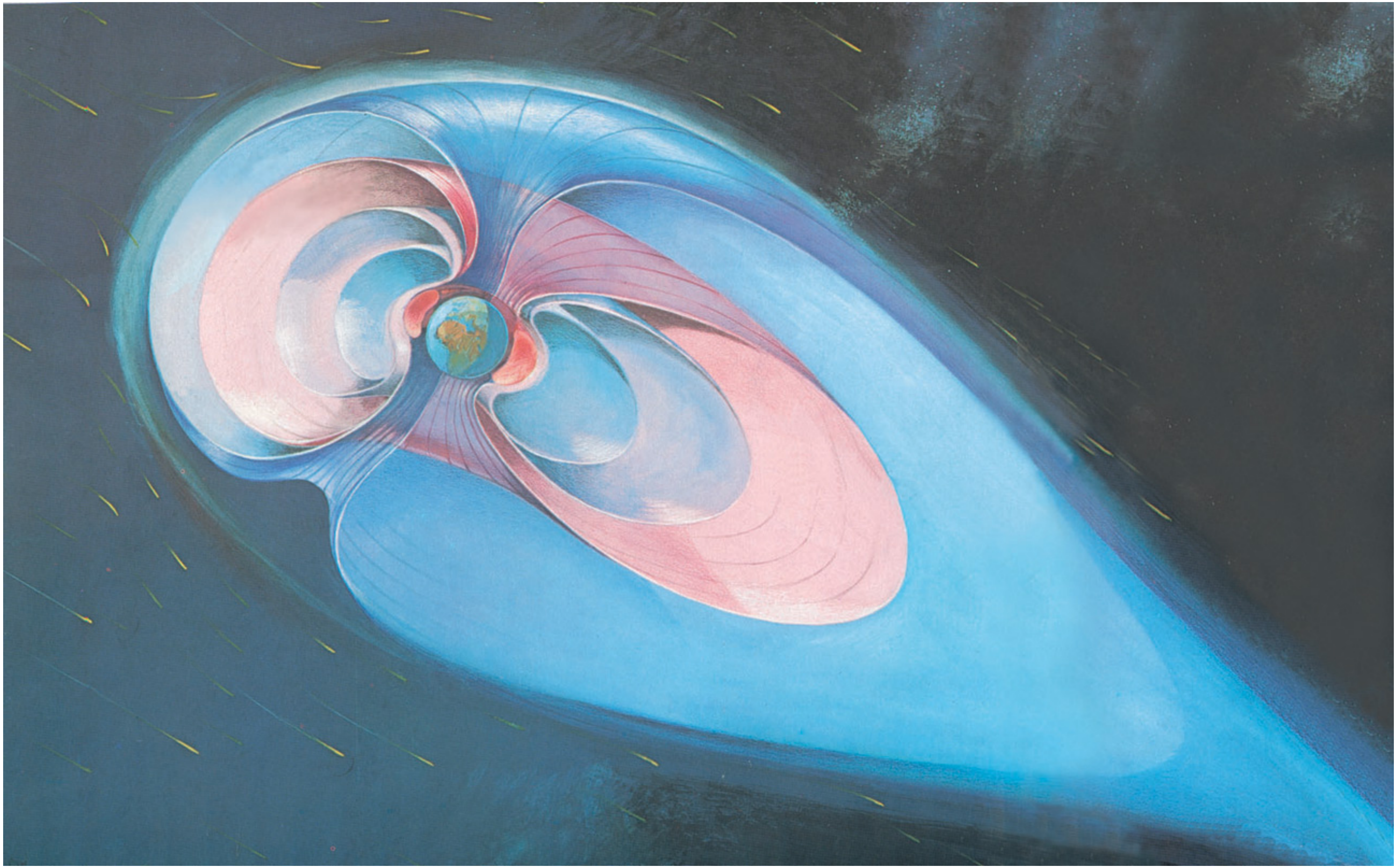

Solar wind influence

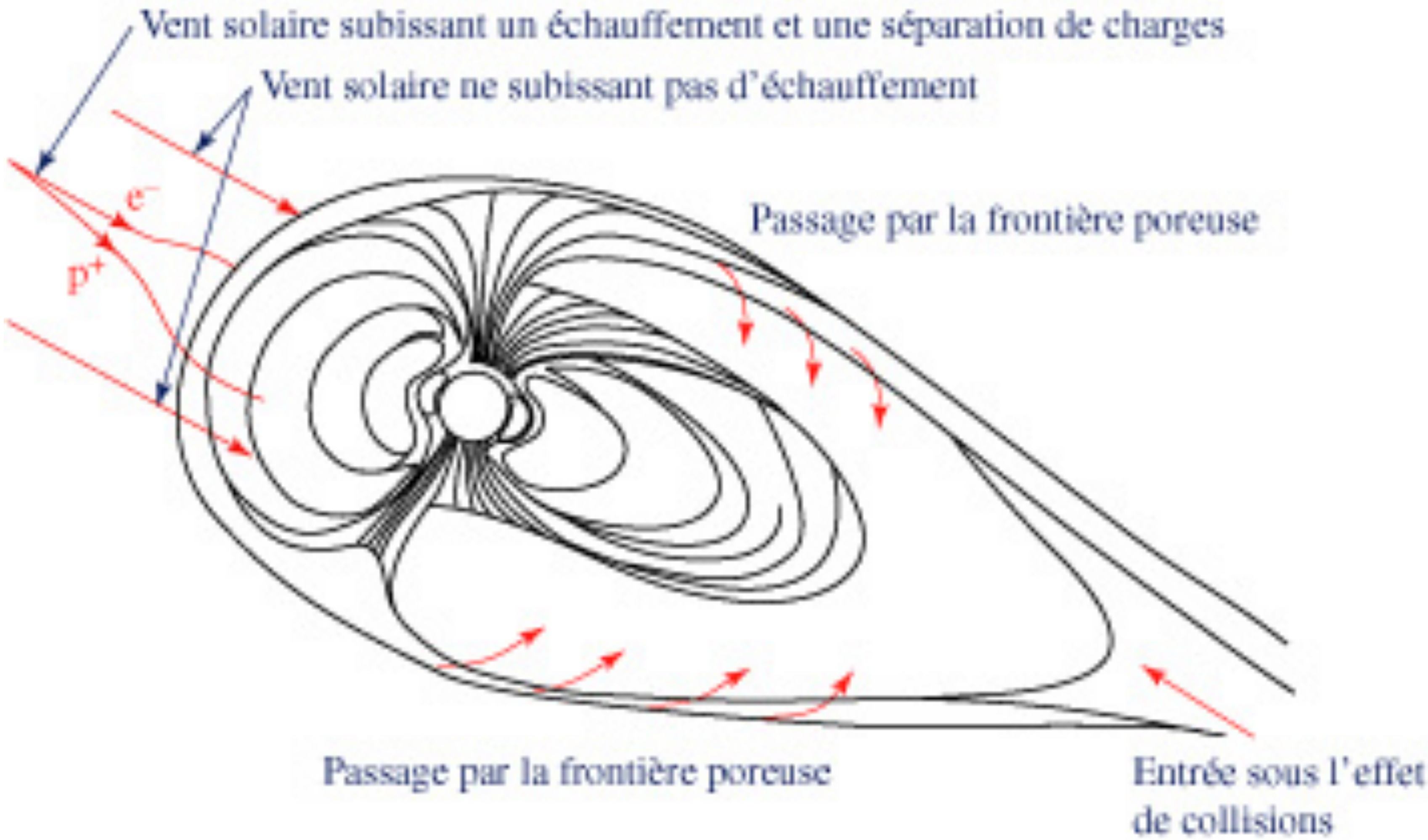

Polar Cusps

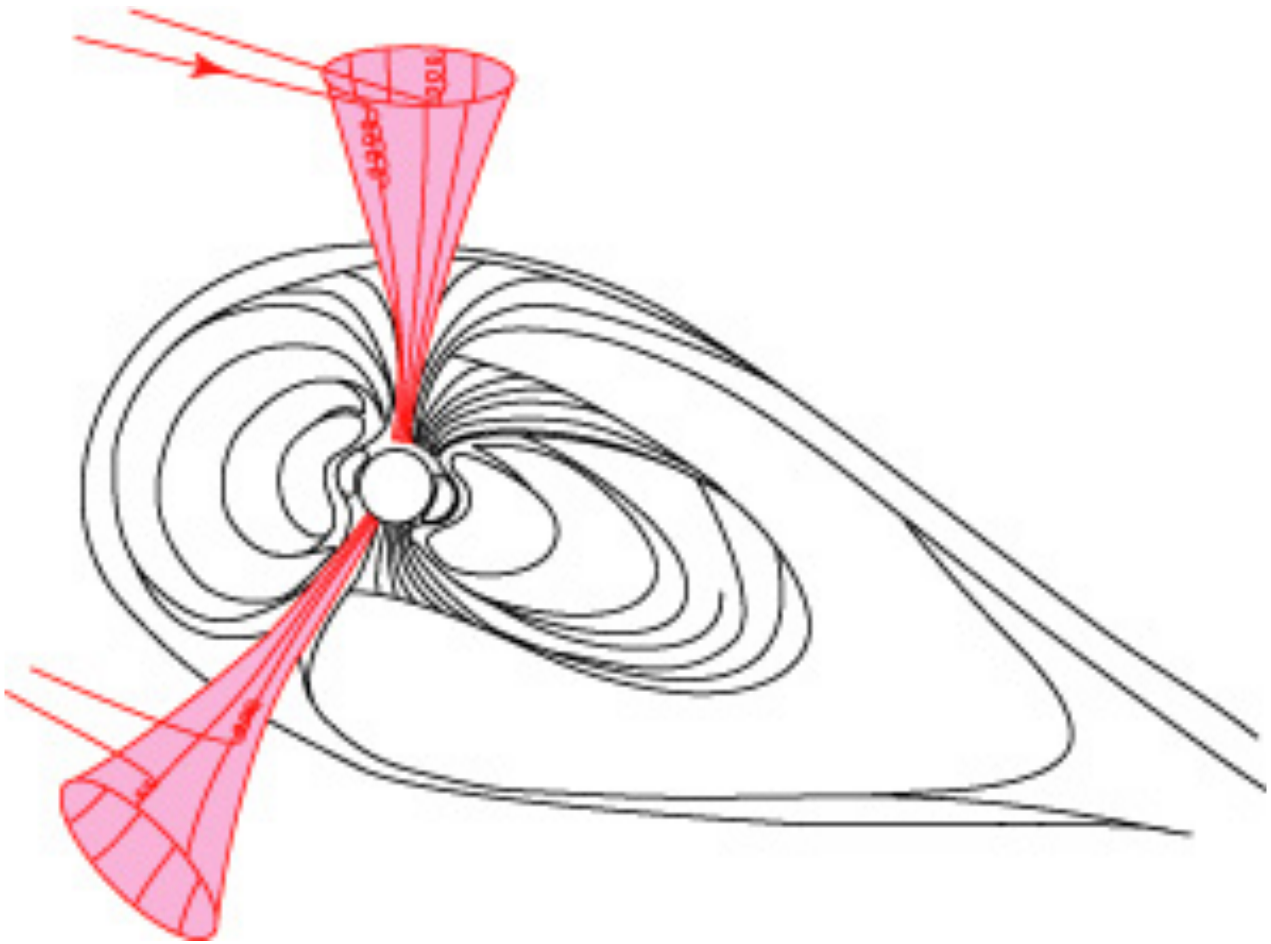

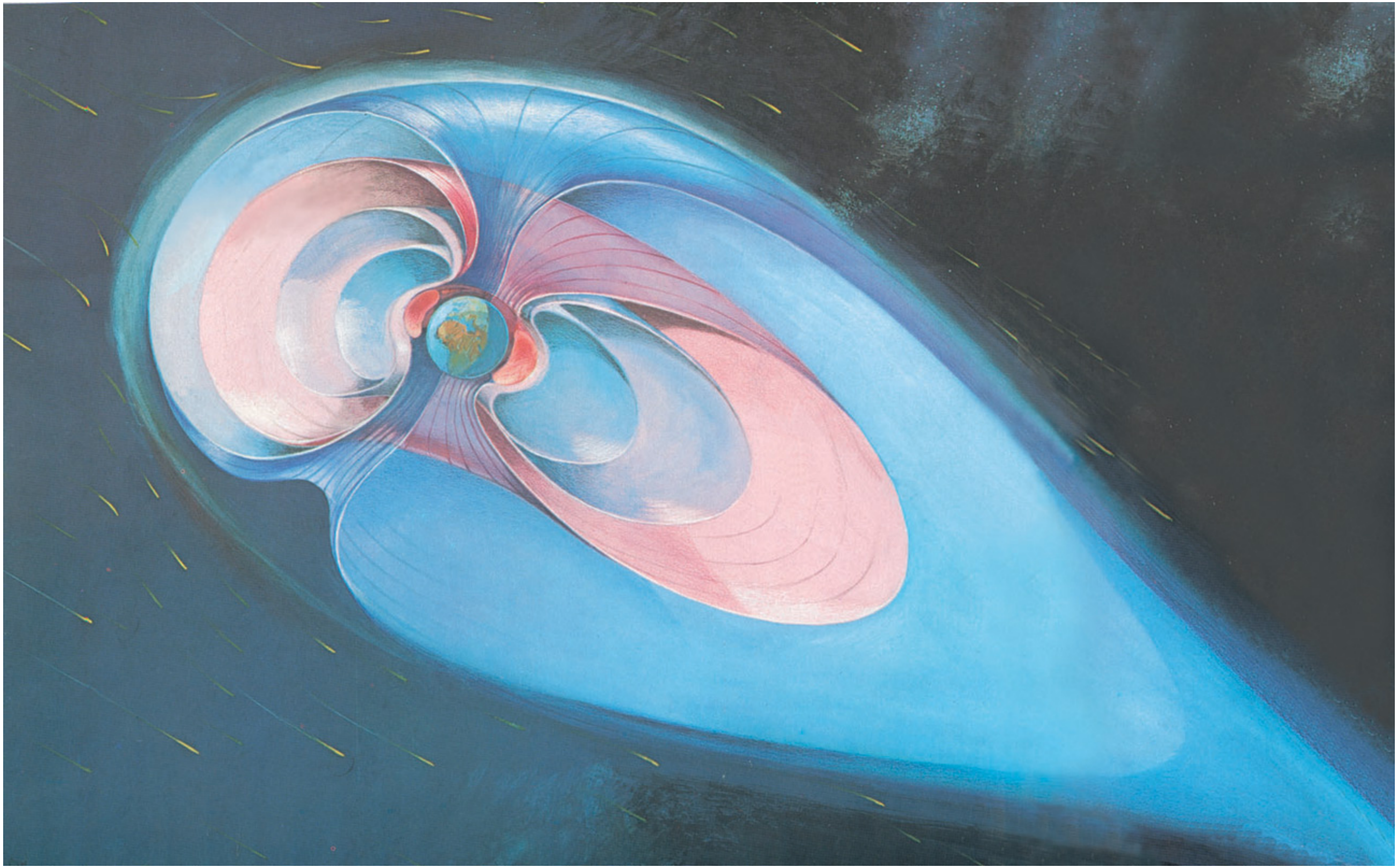

La magnétosphère interne.

Radiation belts

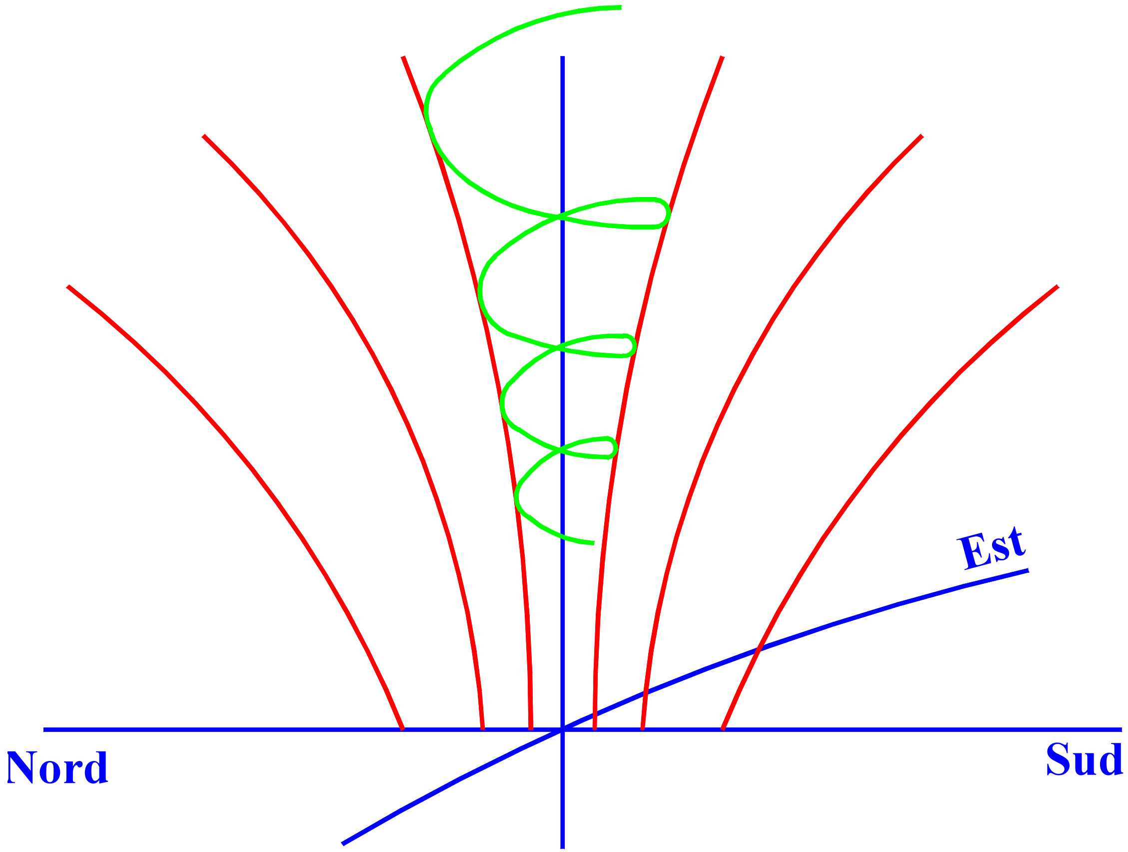

Magnetic mirror geometry.

Auroral oval

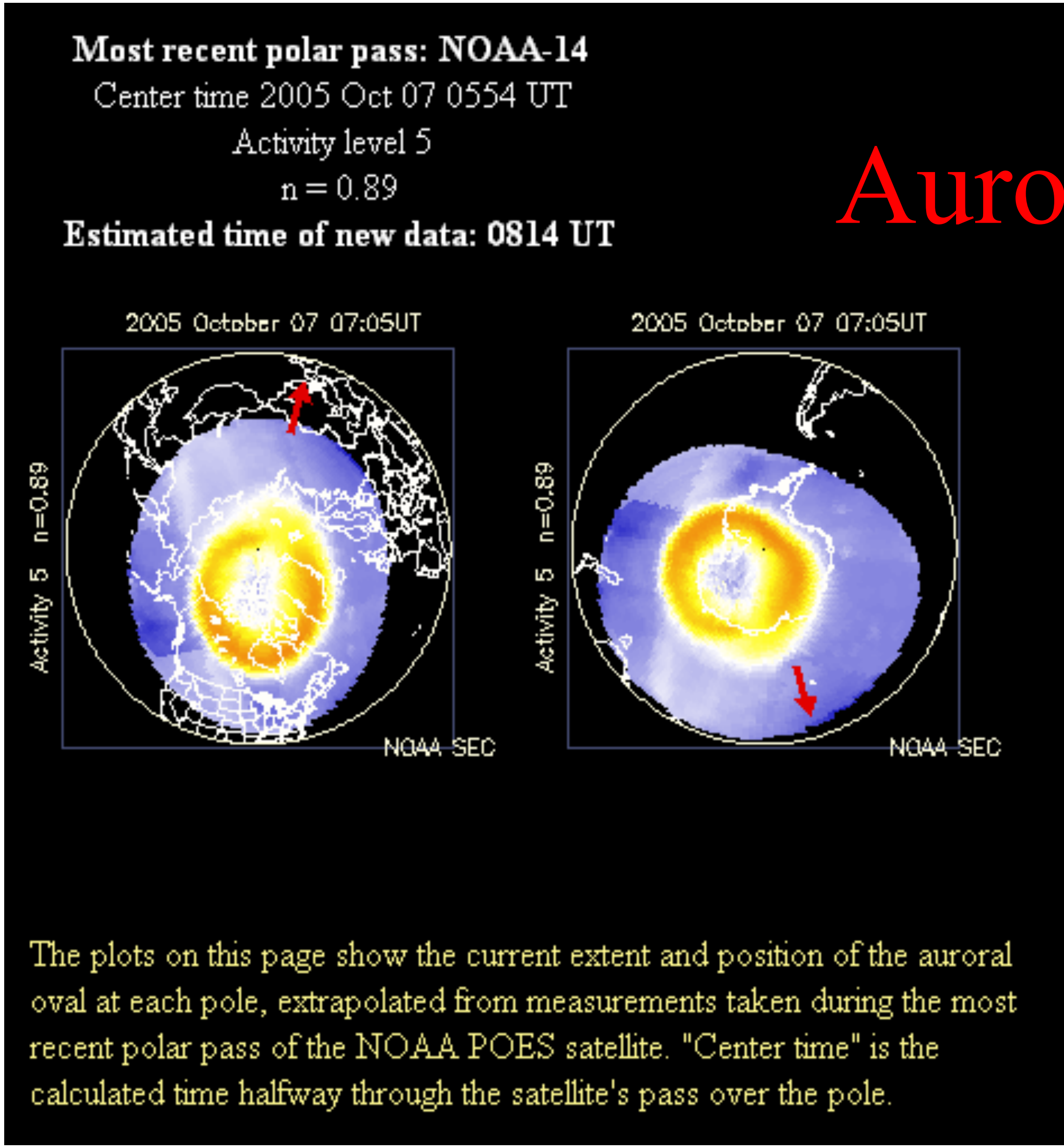

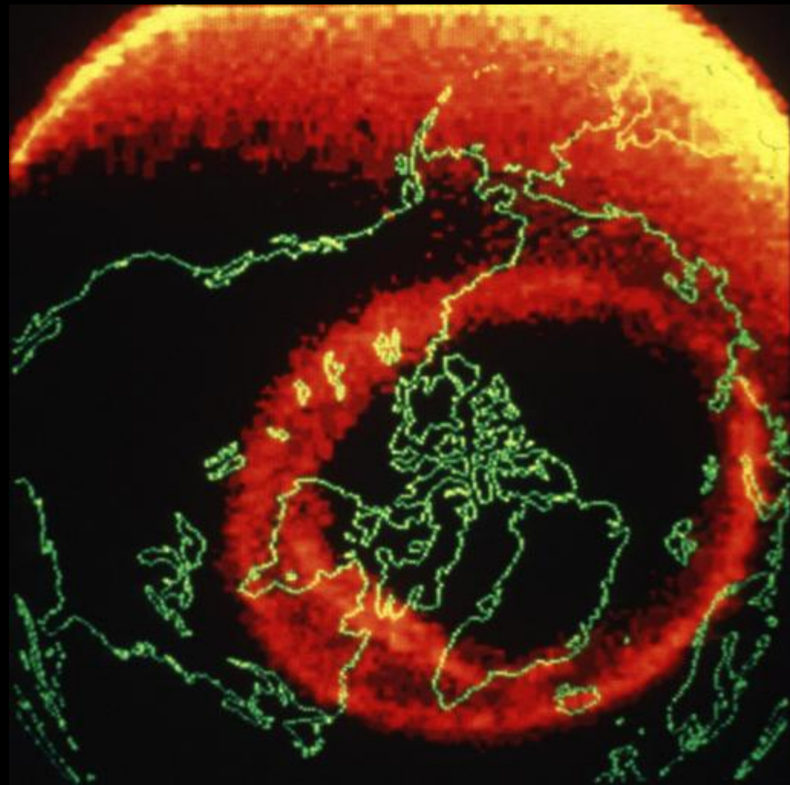

Auroral oval taken from dynamic explorer.

Atmoshpere magnetosphere interaction

- Particles precipitation
  - Electrons
    - – Data from DMSP satellites
      - » 2 populations with a separation around 600 eV

<u>pop : E>600eV</u> →More energetic on the dawn side.

→ 2 maxima just before noon and midnight .

Mean Energy around 3.5 keV; fluxes ~1.5×10^{8}keV.cm².s-1.sr-1 for Kp=1

<u>pop : E<600eV</u>

→closer to the pole. More important on the dayside.

→Mean energy around 220eV for Kp=1

Question of the distribution

Distribution maxwellienne : $F(E) = \alpha_1 e^{-\frac{E - E_{moyenne}}{\gamma_1}}$

Distribution gaussienne : $F(E) = \alpha_2 e^{-\frac{(E - E_{moyenne})^2}{\gamma_2}}$

Atmosphere magnetosphere interaction.

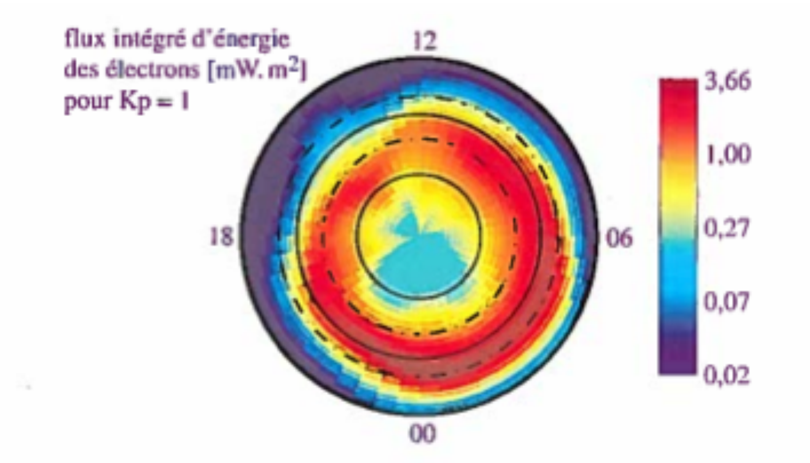

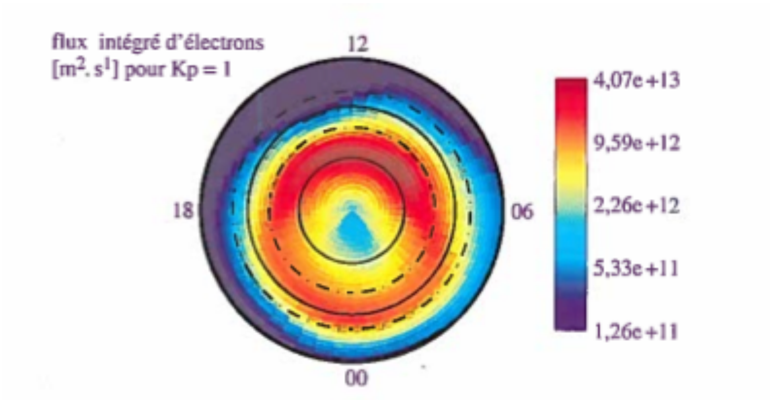

Figure *I-2* : Oval model for Kp=1. Statistical model based on dynamic explorer (Hardy D.A., M.S. Gussenhoven , and E. Holeman, A statistical model of auroral electron precipitation., *J. Geophys. Res.*, 90, A5, 4229-4248, 1985). Left panel: integrated energy flux (mW.m^{-2}). Integrated particle flux [s^{-1}.m^{-2}].

Atmospher magnetosphere interaction

- ions

DMSP spectra: 26 millions
- Max ~24h and min ~12h. Max Mean energy ***13,6* keV** energy flux ***5,52*** $\boldsymbol{10^7}$ **keV cm-*2* s-*1* sr-*1***. Kp=1
Diurnal minimum, mean Energy ***2,54* keV** ; flux ***1,23*** $\boldsymbol{10^7}$ **keV cm-*2* s-*1* sr-*1***.

-NB: Plasmasphere connection induces precipitation at low latitude also. However they are 1000 times weaker.


Emissions processes?

Terrestrial atmosphere: composition and fluid nomenclatura.

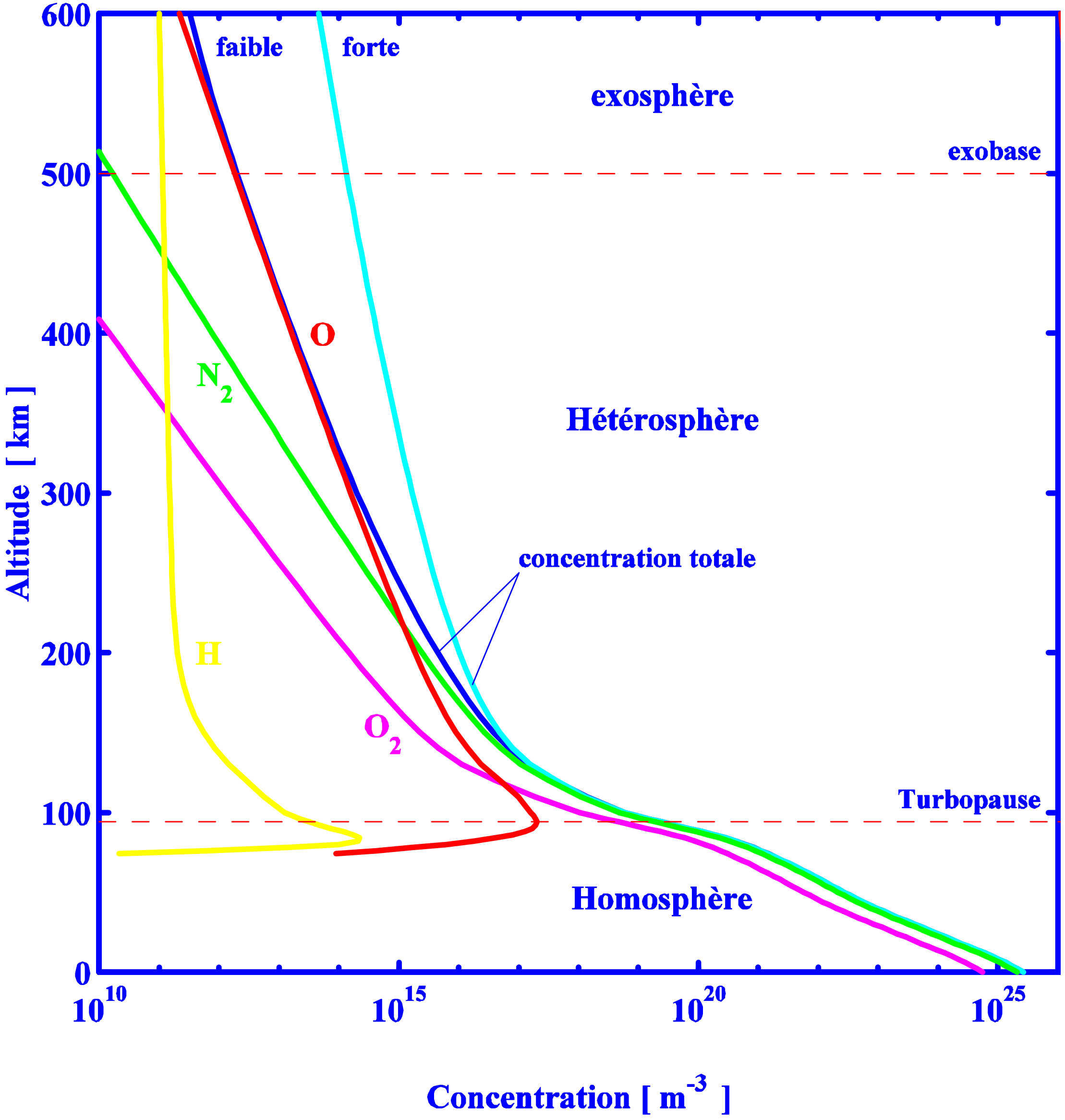

Atmosphere and ionosphere.

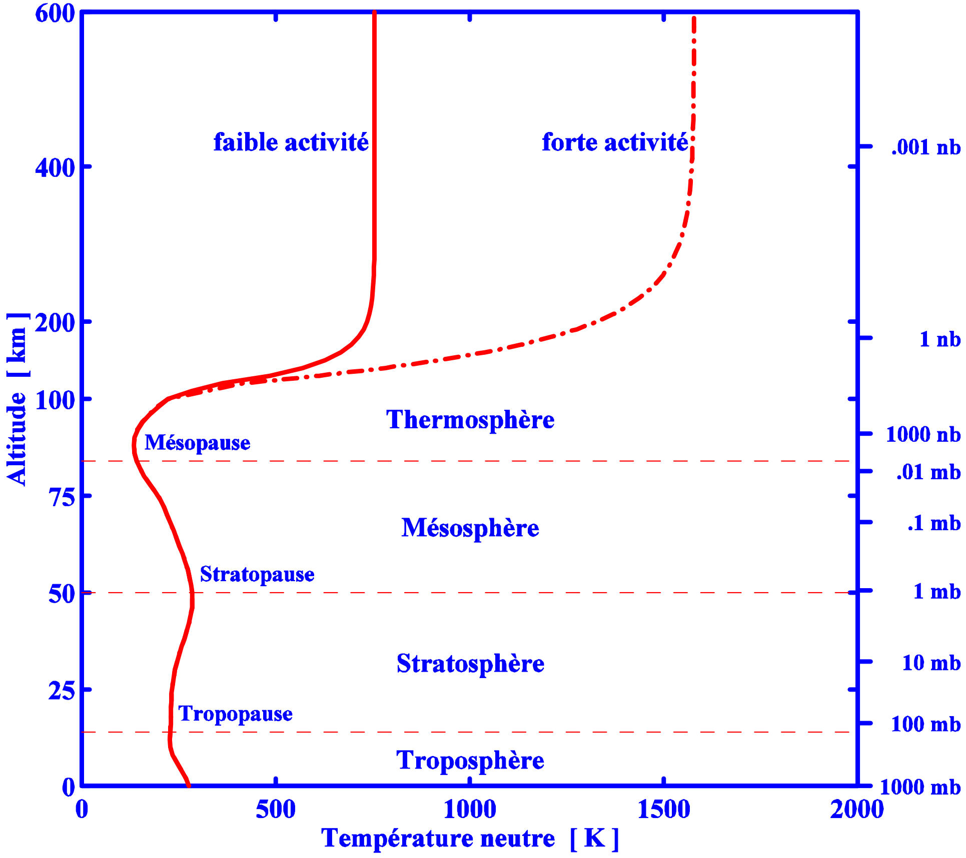

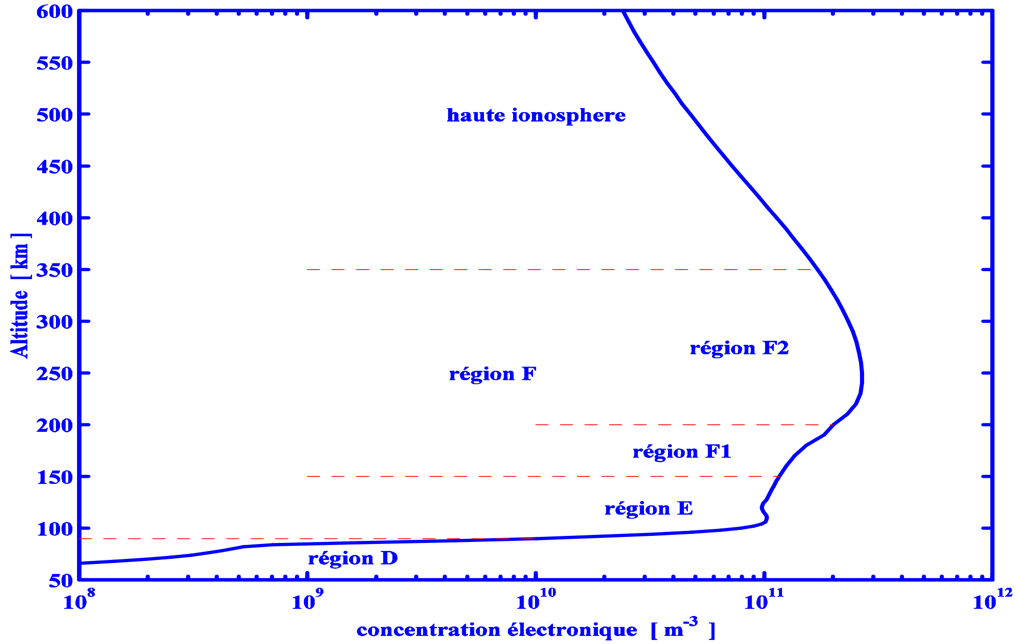

Spectrum.

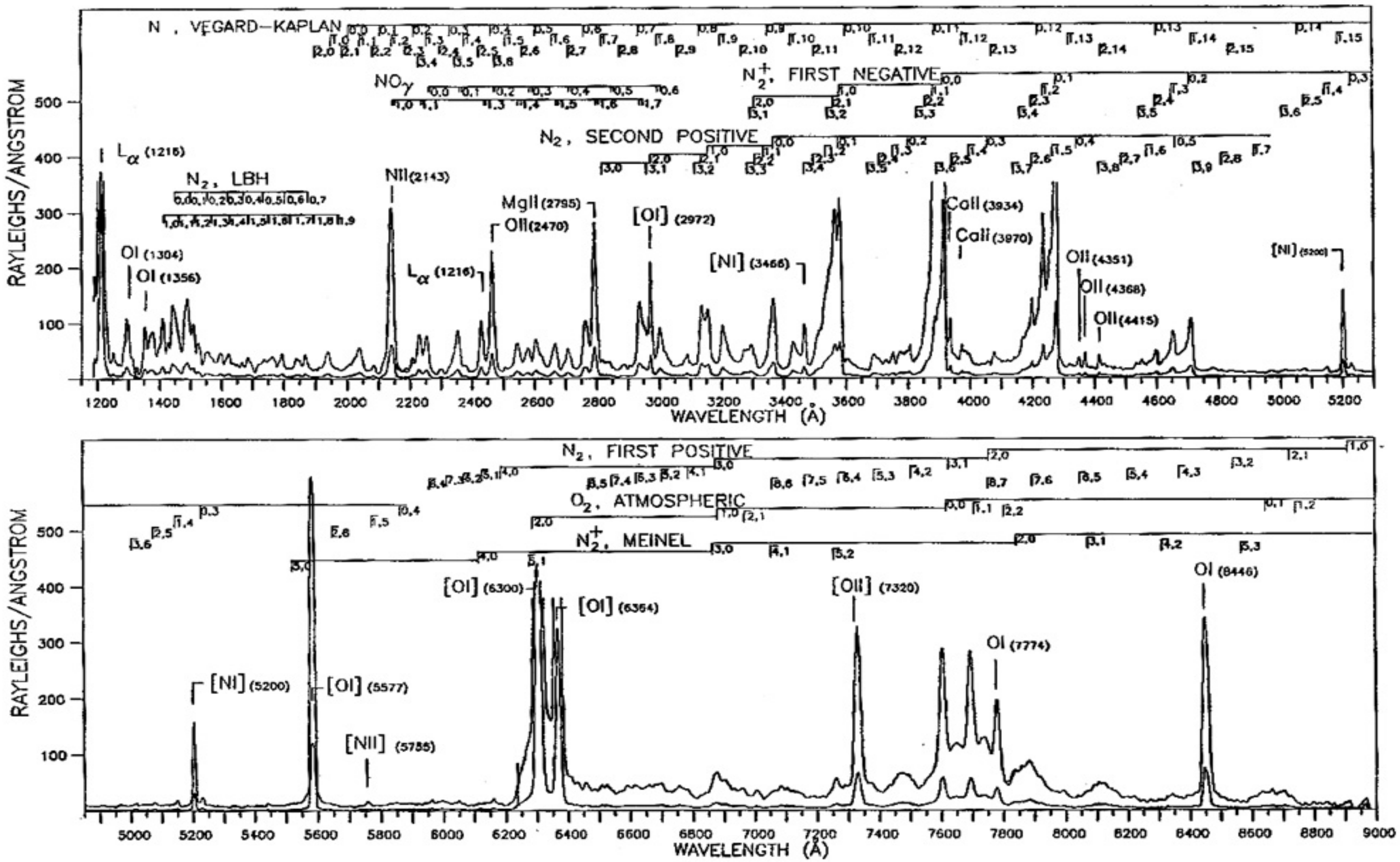

Spectrum of the airglow. Sza= 48°, f10.7= 80. from Broadfoot et al. 1997

Solar EUV flux vs electron precipitation

- Chapman theory
  - SZA

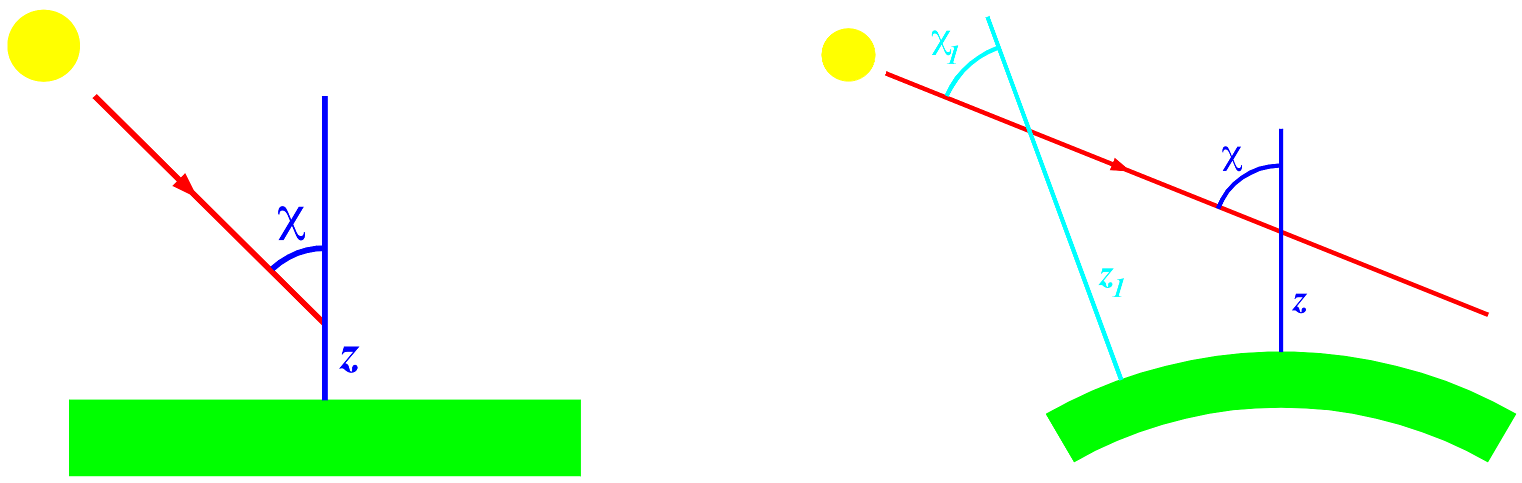

Electron production

$$P(z) = \sigma_i\, n_n^{\,o} \exp\left\{ -\frac{z-z_o}{H_n} - \frac{\sigma_a\, n_n^{\,o}\, H_n}{\cos\chi}\, \mathrm{e}^{-\frac{z-z_o}{H_n}} \right\} \Im_\infty$$

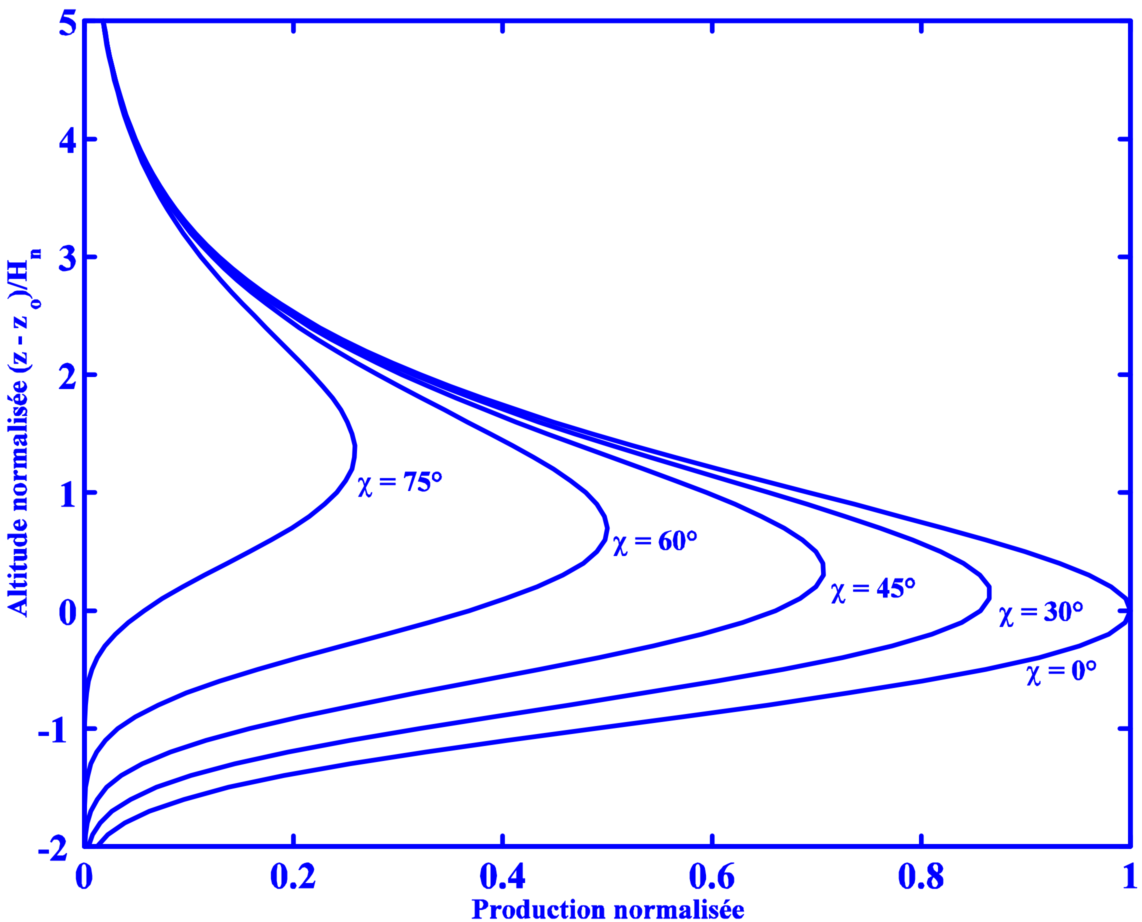

Electron concentration

$$n_e(z) = \sqrt{\frac{P_o}{\alpha}} \exp \frac{1}{2}\left\{ 1 - \frac{z-z_o}{H_n} - \frac{1}{\cos\chi}\, \mathrm{e}^{-\frac{z-z_o}{H_n}} \right\}$$

Secondary electrons and transport.

- Kinetic calculations
  - Primary: Energetic input (Photons or electrons from the magnetosphere)
  - Secondary: Transport equation (Botzmann)
    - Loss and creation (chemical equilibrium)
- Need for large database of cross sections
  - Pb of the redistribution angles
    - Large question of the double differential cross sections

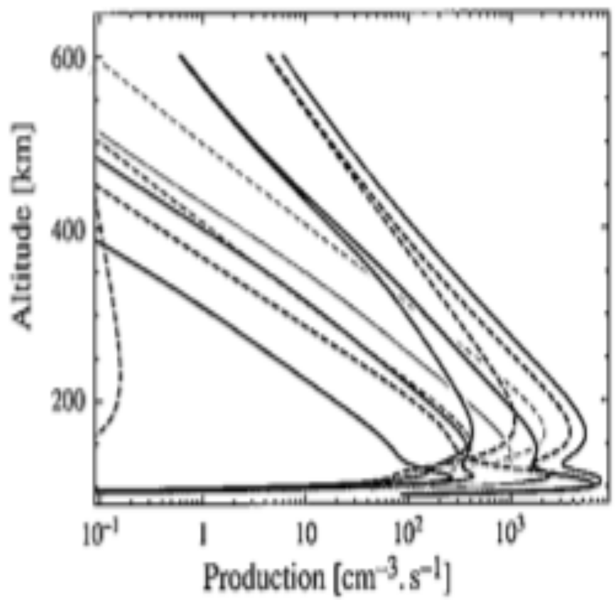

Figure V–8 : sur cette figure, nous avons fait figurer les productions ioniques primaire (en pointillé) et secondaire (en trait plein)
La somme, constituant la production électronique, est montrée en trait gris. N_2^+ est en jaune, O_2^+ en vert et O^+ en bleu clair. Les traits rouges représentent les sommes des productions primaires ou secondaires.

Ionospheric layers

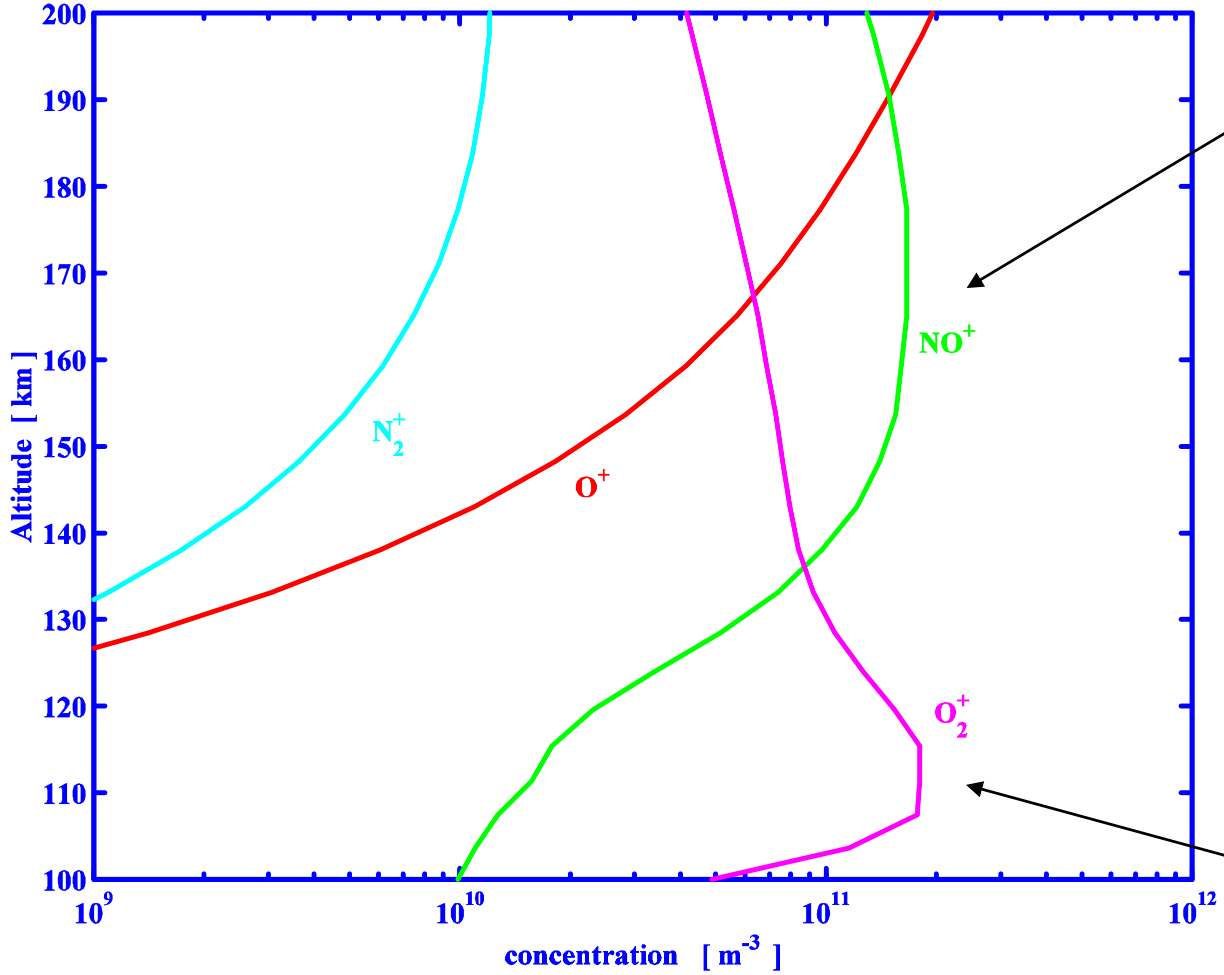

F1 region peak

Dayside Ionosphere χ=80°, f10.7 = 100.

E region peak

Figure *I-17* : vertical profile of the ionic concentrations.

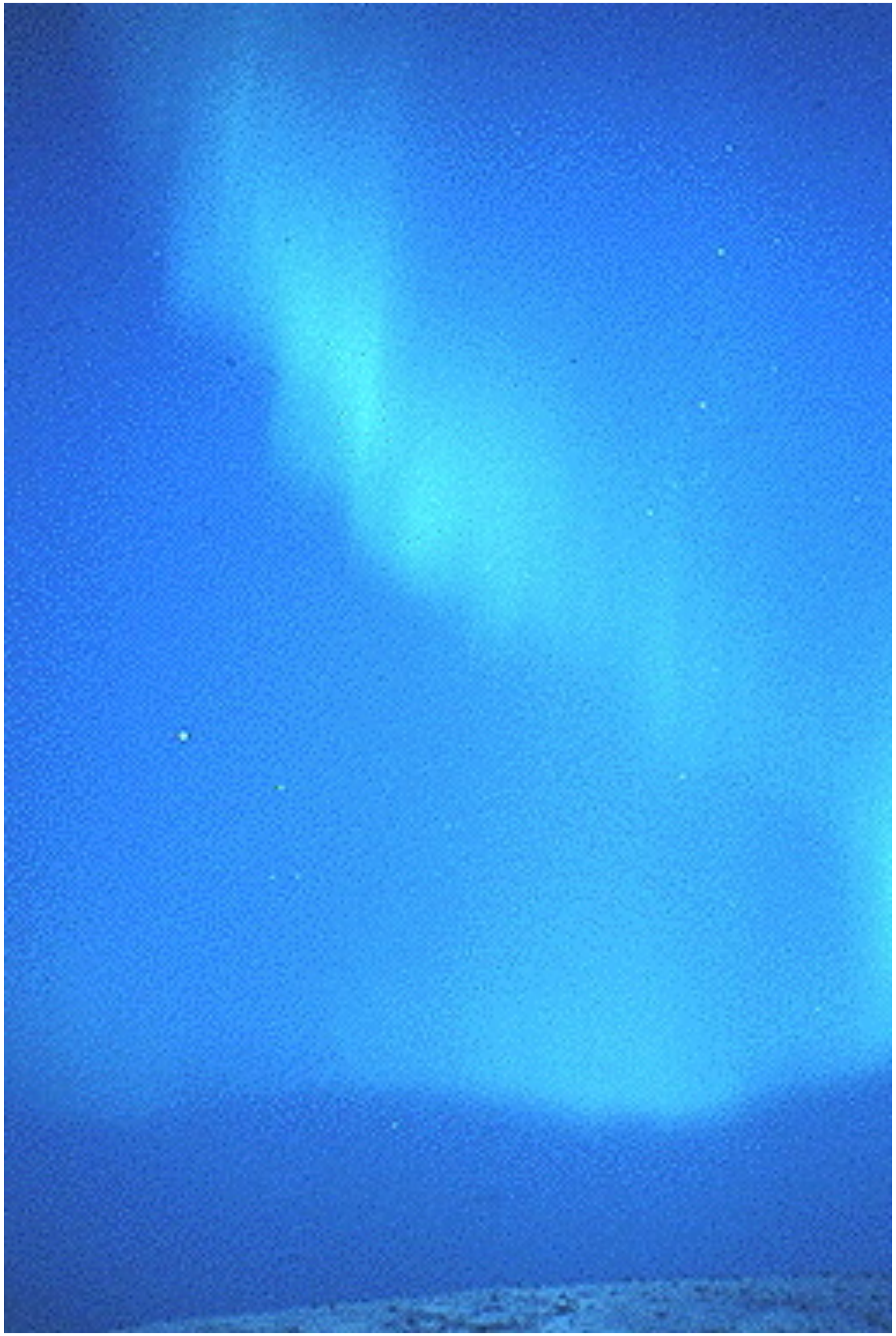

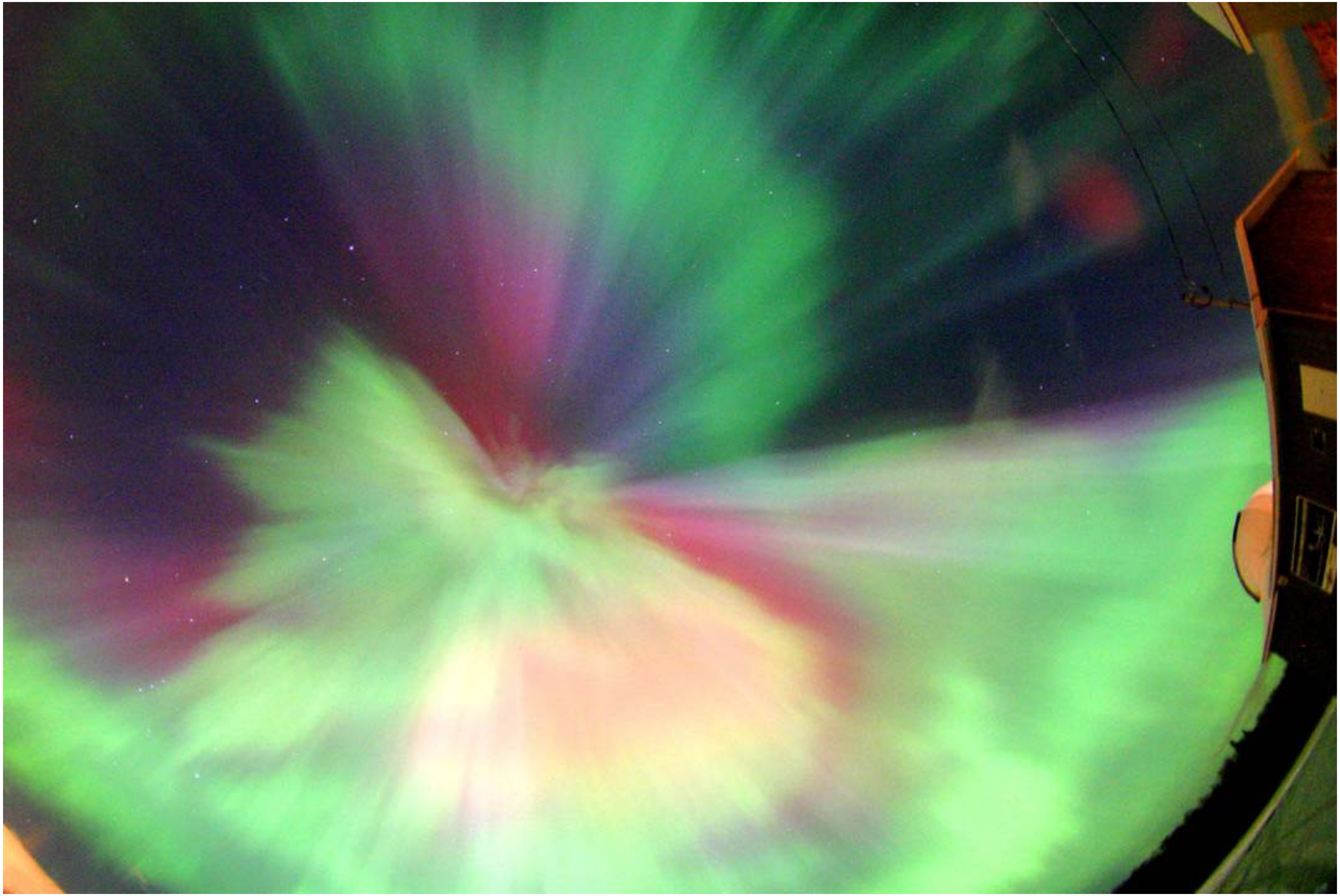


©2000 Laboratoire de Planétologie de Grenoble - France


©2000 Laboratoire de Planétologie de Grenoble - France


©2000 Laboratoire de Planétologie de Grenoble - France


©2000 Laboratoire de Planétologie de Grenoble - France


©2000 Laboratoire de Planétologie de Grenoble - France


©2000 Laboratoire de Planétologie de Grenoble - France

©2000 Laboratoire de Planétologie de Grenoble - France

©2000 Laboratoire de Planétologie de Grenoble - France

©2000 Laboratoire de Planétologie de Grenoble - France


©2000 Laboratoire de Planétologie de Grenoble - France

©2000 Laboratoire de Planétologie de Grenoble - France

©2000 Laboratoire de Planétologie de Grenoble - France

©2000 Laboratoire de Planétologie de Grenoble - France


©2000 Laboratoire de Planétologie de Grenoble - France

©2000 Laboratoire de Planétologie de Grenoble - France

©2000 Laboratoire de Planétologie de Grenoble - France

©2000 Laboratoire de Planétologie de Grenoble - France


© 2000 Laboratoire de Planétologie de Grenoble - France

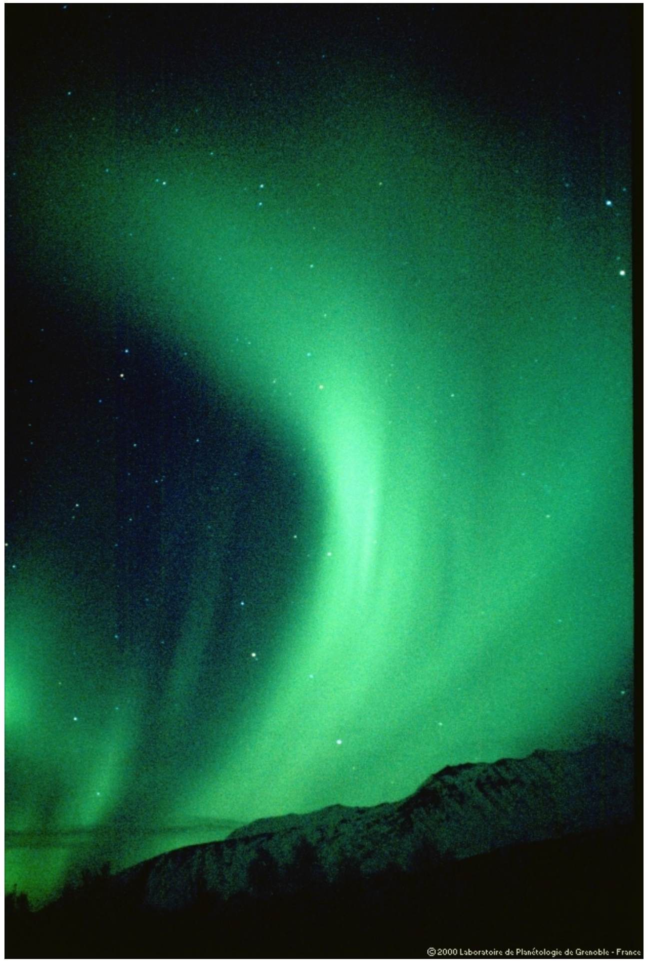
© 2000 Laboratoire de Planétologie de Grenoble - France


© 2000 Laboratoire de Planétologie de Grenoble - France


©2000 Laboratoire de Planétologie de Grenoble - France


©2000 Laboratoire de Planétologie de Grenoble - France


©2000 Laboratoire de Planétologie de Grenoble - France


©2000 Laboratoire de Planétologie de Grenoble - France


LeRoy Zimmerman


LeRoy Zimmerman


LeRoy Zimmerman



© Daniel Girard

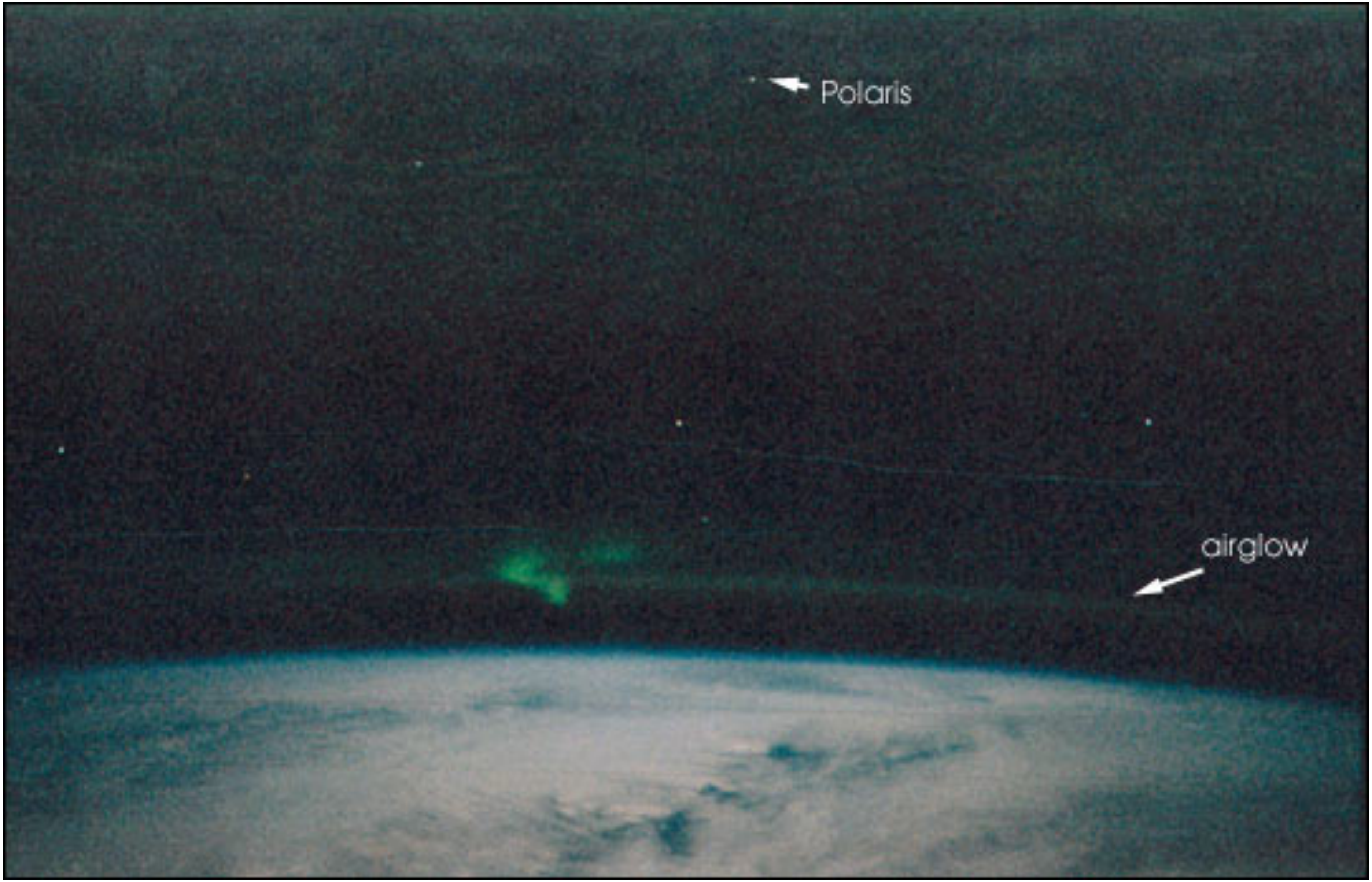
Polaris
airglow

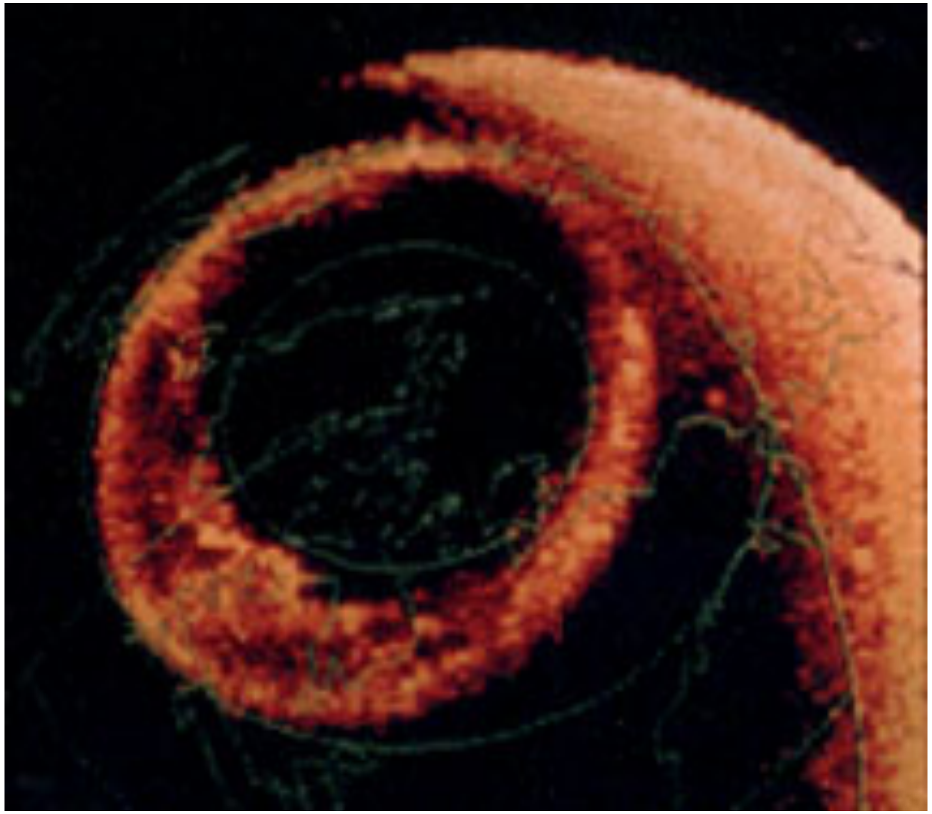

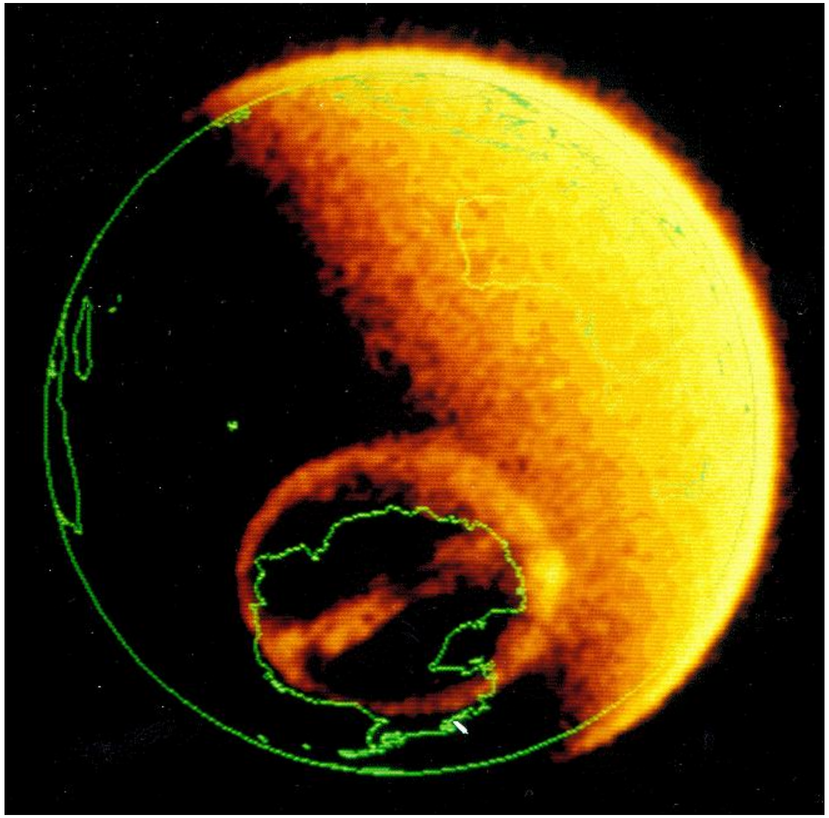

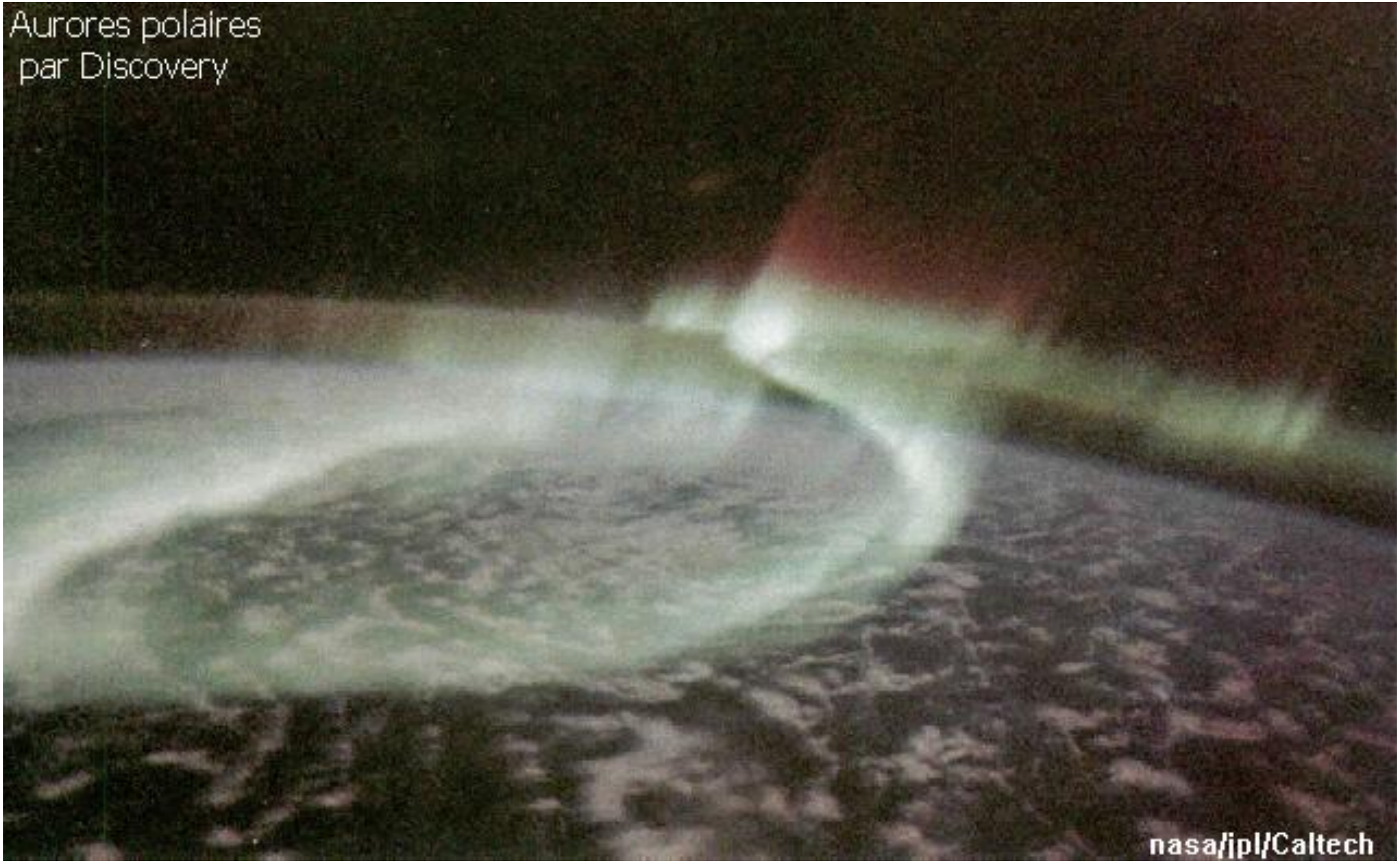
Aurores polaires
par Discovery
nasa/jpl/Caltech

Problematic of the auroral studies?

Lack of observable quantities.

too high for ballons, too low for satellites…

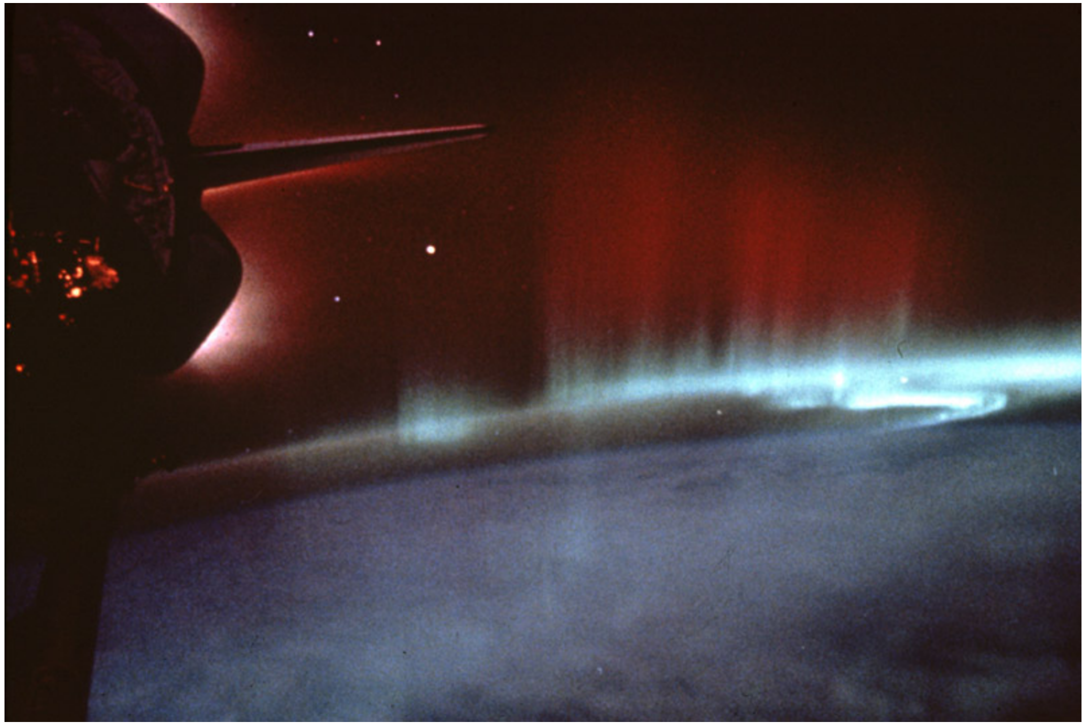

A useful instrument for ionospheric studies.

- Incoherent scaterring
  - $f > f_{plasma}$
  - $\lambda <$ Debye length

  Typically λ_D=0.27cm an thus f_{max}=100 GHz
  - In fact
    - VHF 224 MHz
    - UHF 931 MHz

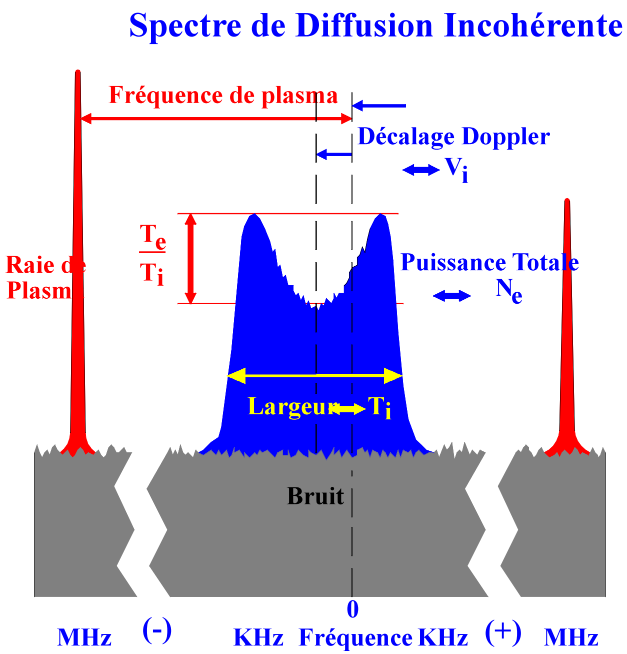

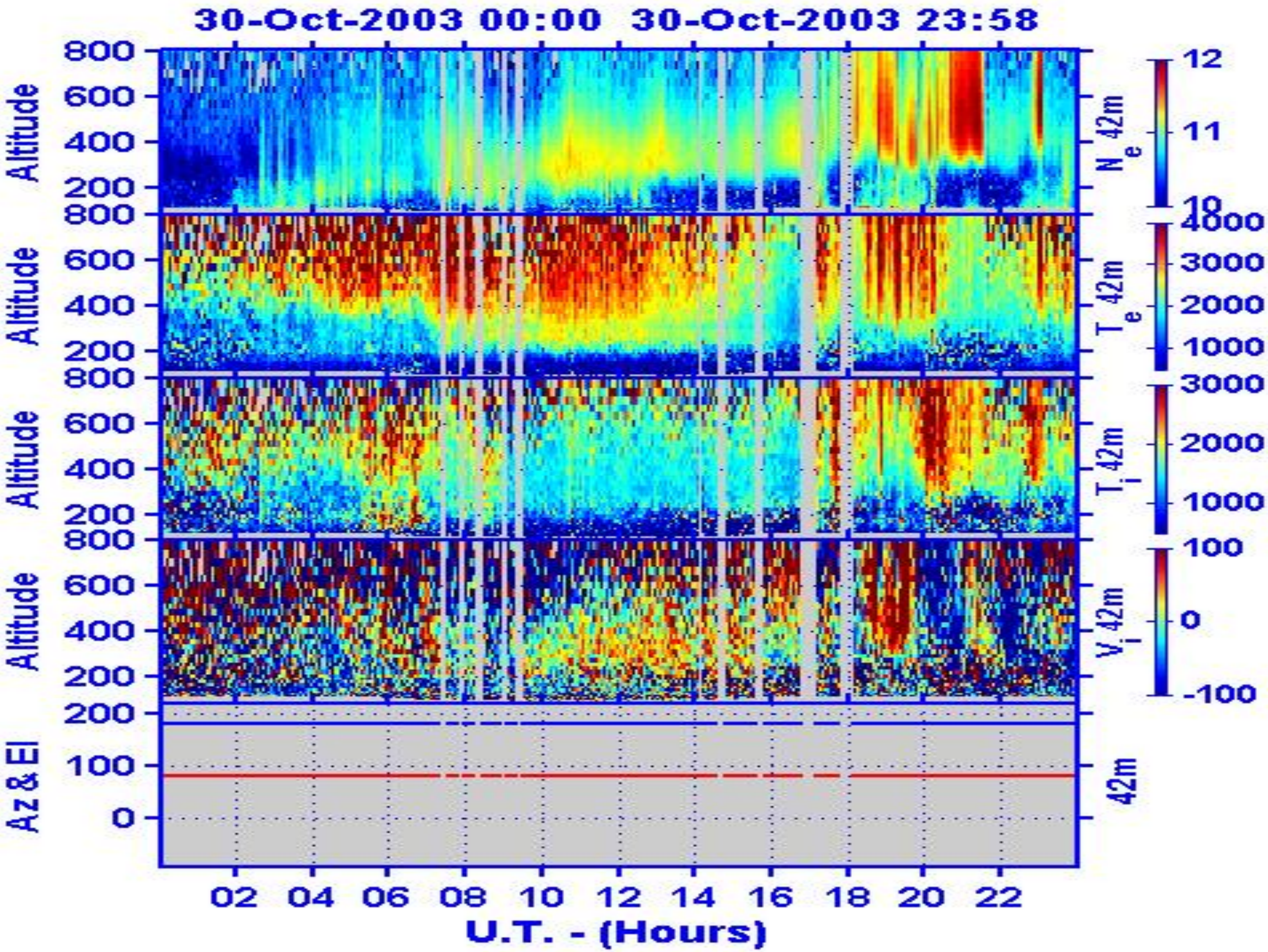

30-Oct-2003 00:00 30-Oct-2003 23:58
Altitude
800
600
400
200
N_e 42m
12
11
10
T_e 42m
4000
3000
2000
1000
T_i 42m
3000
2000
1000
V_i 42m
100
0
-100
Az & El
200
100
0
42m
02 04 06 08 10 12 14 16 18 20 22
U.T. - (Hours)

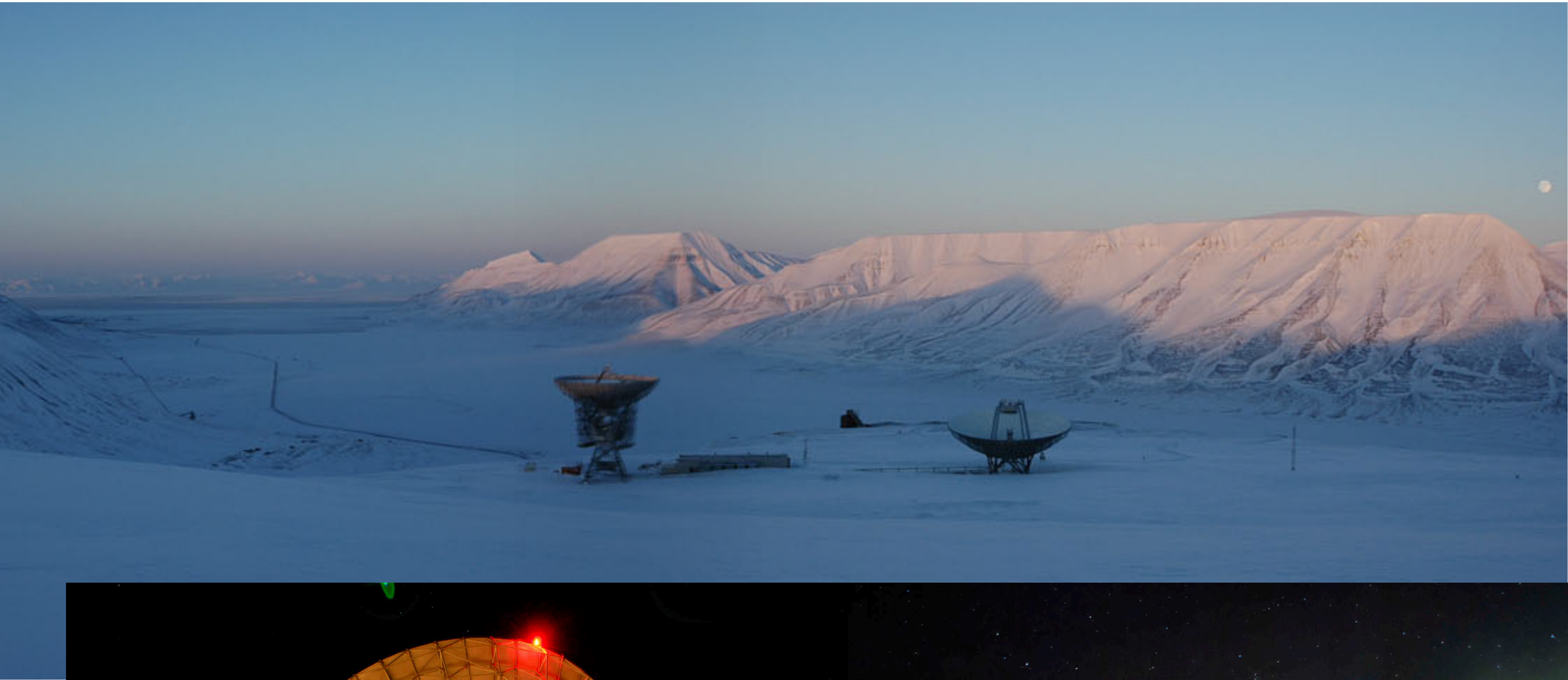

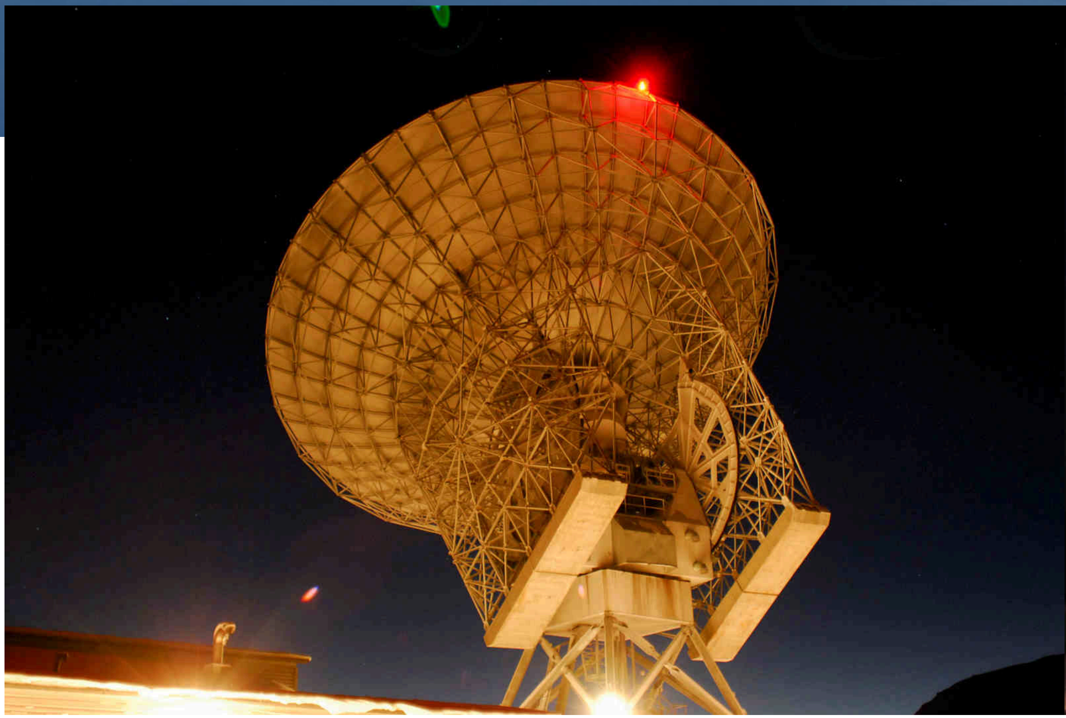

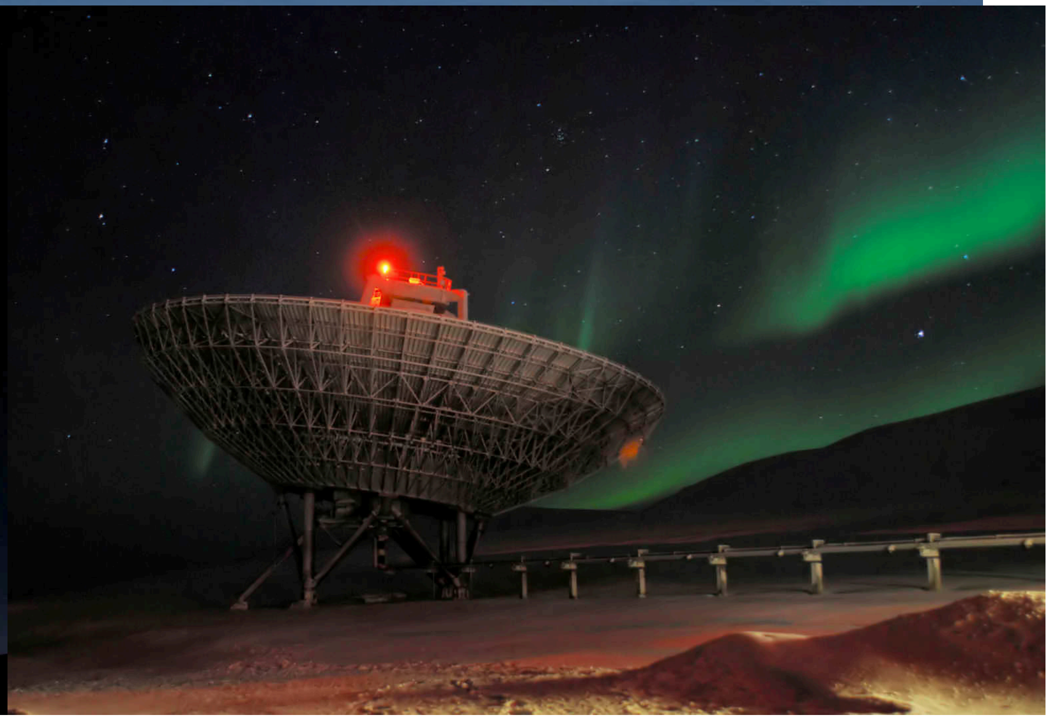

Spectral data

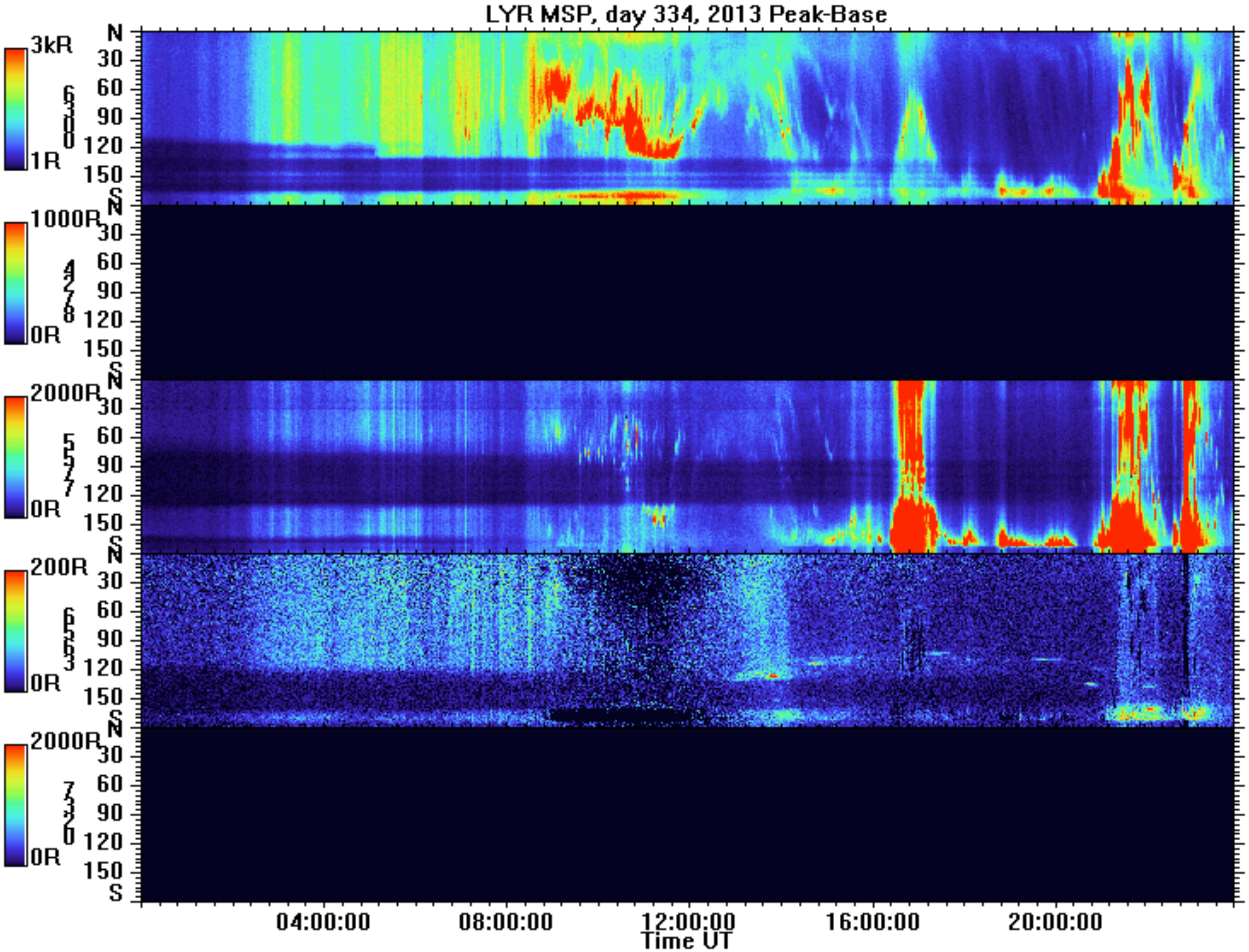

But still missing data.

Polarisation of the emission

SPP: technical details

- Photopolarimeter: SPP.

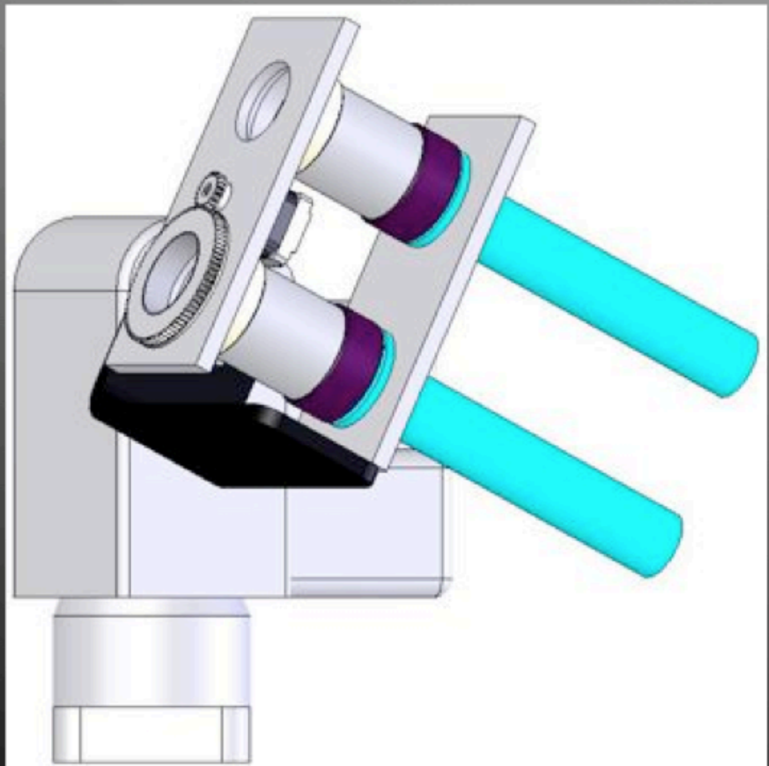

Steerable Polarization Photometer (SPP) built at Oslo University (UIO).

<u>Channel 1</u>: PM.

Red filter at 630 nm (FWHM 1 nm.

Rotating Analyser (T=4s)

Field of view 2°

Instrumental polarisation <0.9%; almost vertical.

<u>Channel 2</u>: Idem without analyser

Polarisation of the emissions

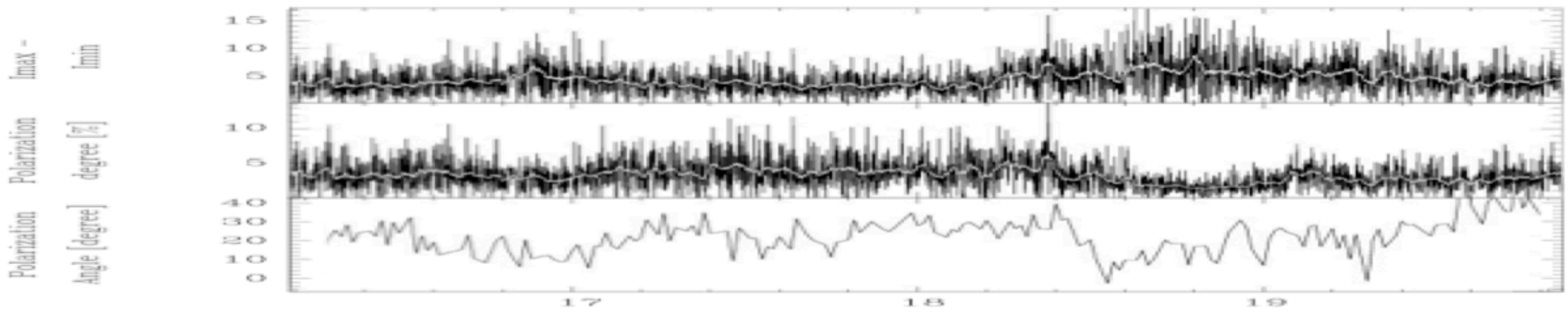

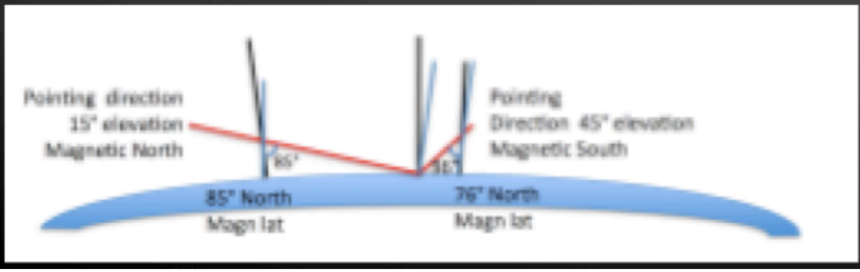

17 jan 2007 late afternoon. From Lilensten et al. 2008. GRL

Polarisation of the emissions

Table 1. Summary of the influence of the parameters on the DoLP. The first column explains the changes versus the test case (which is given in the first line). The Altitude (in km) in column 2 is the one where the DoLP maximizes with the variation (in %) versus the test case in the third column. The DoLP in the fourth column is the maximum value with its variation (in %) versus the test case. In the next column, the DoLP is integrated over all the altitudes and finally the variation of this integral average versus the test case. The last column gives the figure that this refers to.

Change vs test	Alt	%	max	%	int	%	Fig.
	213		1.79		0.62		8
Only thermal e^-	186	-12.7	0.	-	0.001	-	-
Only supra therm.	213	0	1.79	0	0.62	0	-
Isotropic ph. fct.	325	52.6	0.58	-67.6	0.46	-25.5	9
Forward ph. fct.	208	-2.3	2.03	13.4	0.63	1.6	9
$[O]/2$	193	-9.4	1.99	11.2	0.76	22.6	10
$[O]*2$	244	14.6	1.77	-1.1	0.51	-17.7	10
$[N_2]/2$	208	-2.3	1.81	1.1	0.58	-6.4	10
$[N_2]*2$	217	1.9	1.83	2.2	0.68	9.7	10
$[O_2]/2$	213	0	1.76	-1.7	0.61	-1.6	10
$[O_2]*2$	213	0	1.83	2.2	0.64	3.2	10
Storm	243	14.1	1.76	-1.7	0.77	24.2	10
1 erg prec.	213	0	1.79	0	0.62	0	-
$[N_e]/2$	213	0	1.83	2.2	0.64	3.2	11
$[N_e]*2$	209	-1.9	1.73	-3.4	0.60	-3.2	11
$T_e/2$	213	0	1.79	0	0.62	0	11
T_e*2	209	-1.9	1.89	5.6	0.61	-1.6	11
Isotropic prec.	221	3.8	2.07	15.6	0.75	21.0	12
Polar rain	225	5.6	2.34	30.7	0.69	11.3	12

Lilensten et al. 2014; submitted to JSWSC

Solar wind effect on the Earth: A step to the space weather.

And on the other planets

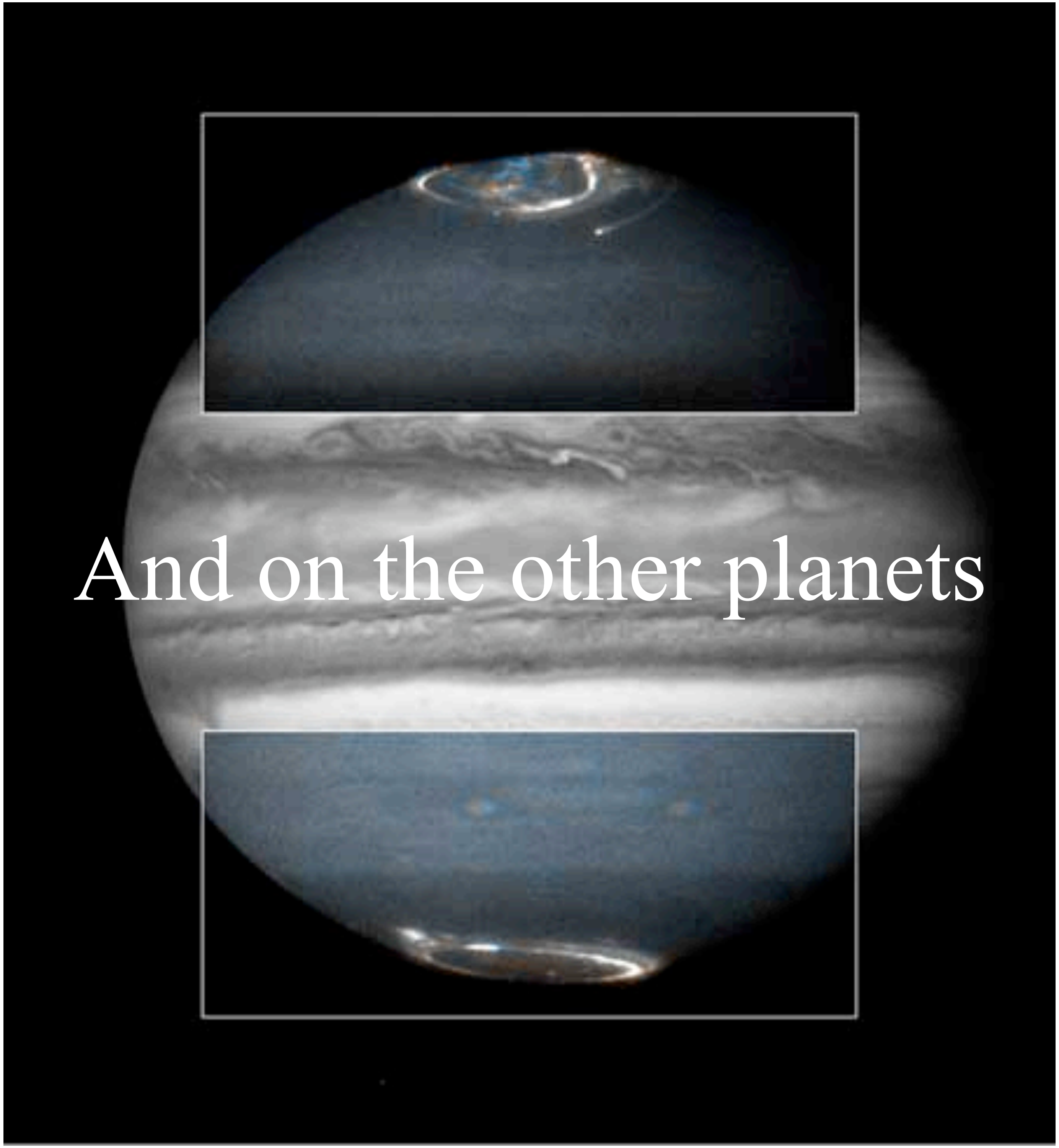

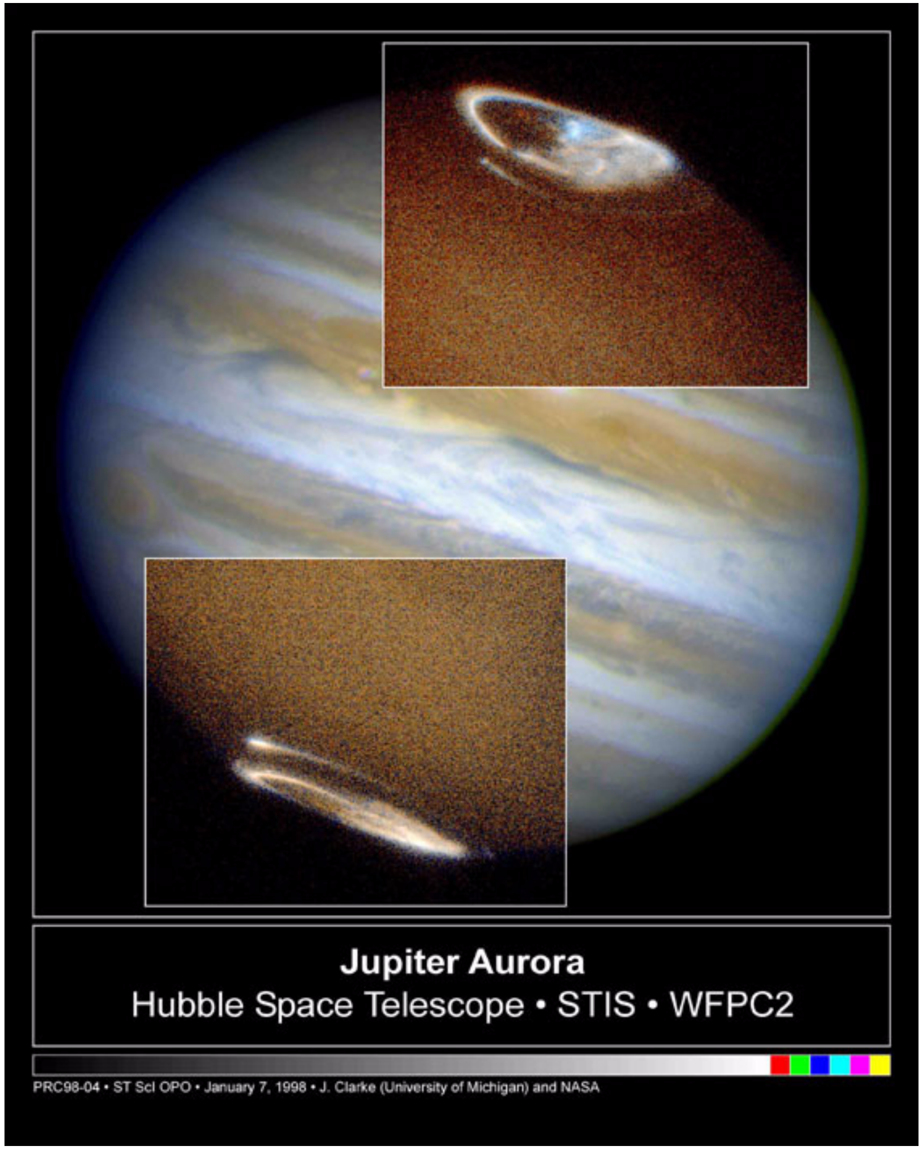
Jupiter Aurora
Hubble Space Telescope • STIS • WFPC2
PRC98-04 • ST ScI OPO • January 7, 1998 • J. Clarke (University of Michigan) and NASA

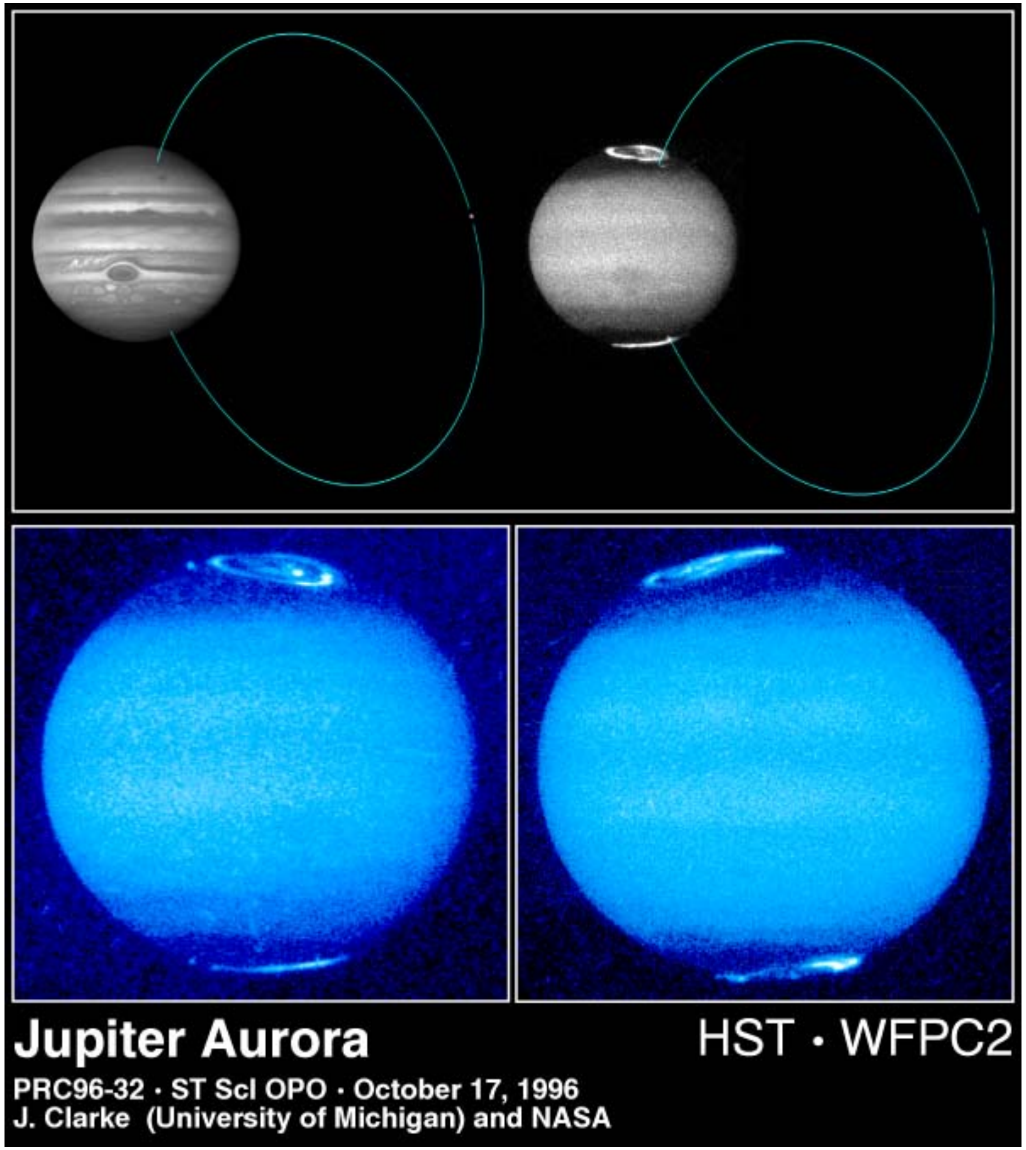
Jupiter Aurora
HST • WFPC2
PRC96-32 • ST ScI OPO • October 17, 1996
J. Clarke (University of Michigan) and NASA

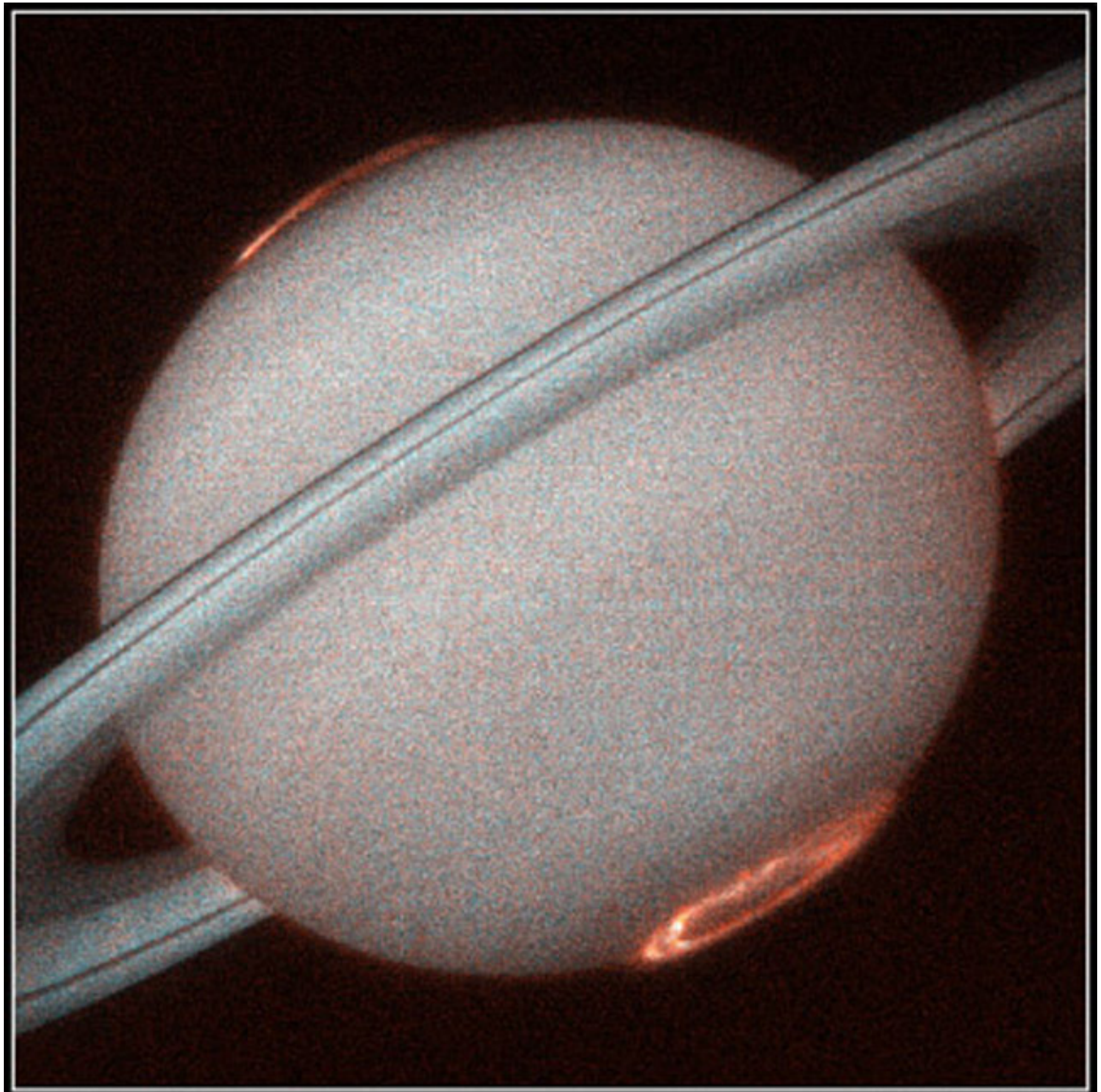

Saturn Aurora HST • STIS
PRC98-05 • ST ScI OPO • January 7, 1998 • J. Trauger (JPL) and NASA

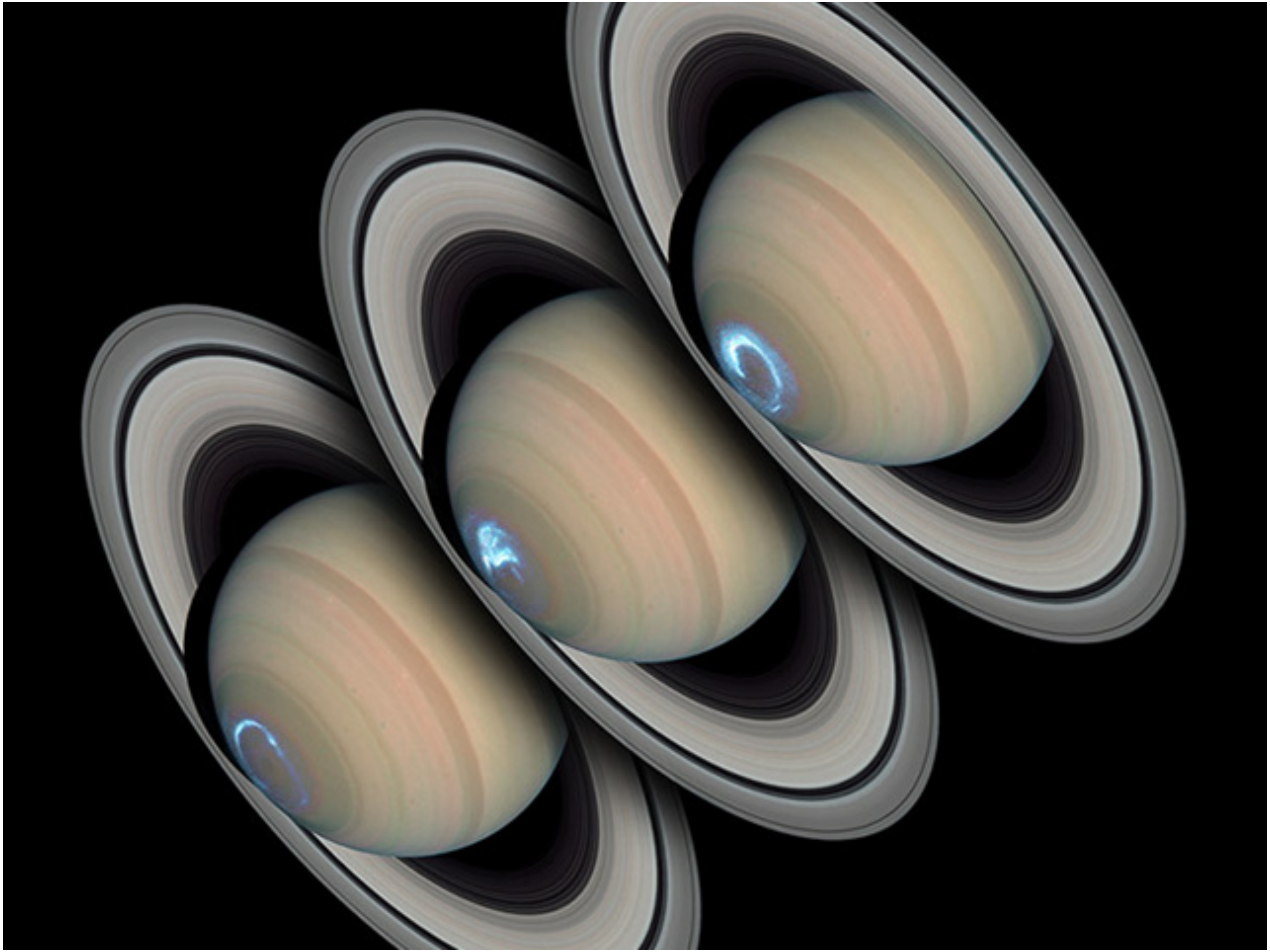

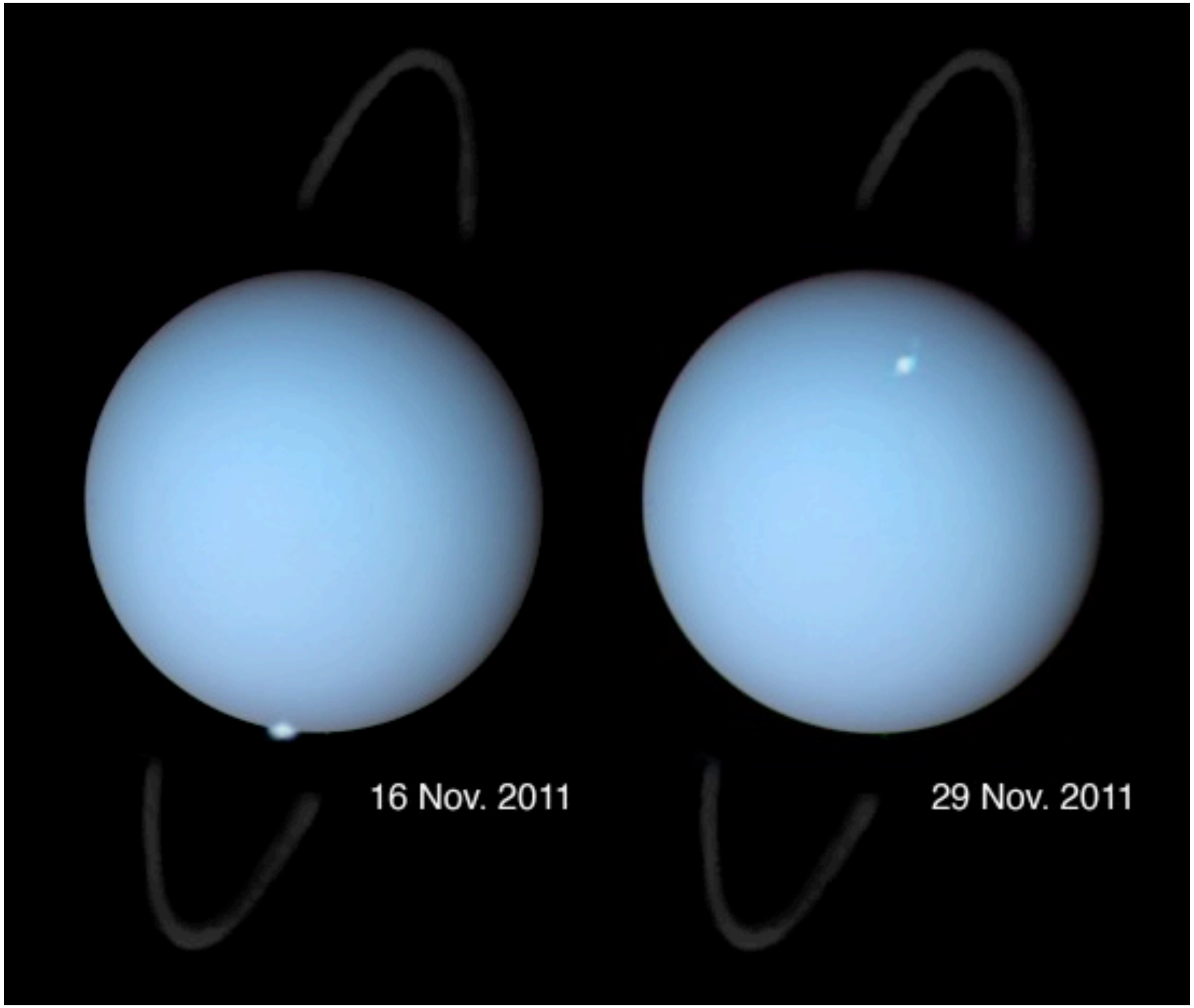

HST STIS detection:
First detection from Earth based telescope.

A very special morphology

The exoplanets?

SEARCHING FOR FAR-ULTRAVIOLET AURORAL/DAYGLOW EMISSION FROM HD209458B.*

KEVIN FRANCE[1], JOHN T. STOCKE
Center for Astrophysics and Space Astronomy, 389 UCB, University of Colorado, Boulder, CO 80309

HAO YANG, JEFFREY L. LINSKY
JILA, University of Colorado, Boulder, CO 80309

BRIAN C. WOLVEN
Applied Physics Laboratory, Johns Hopkins University, 11100 Johns Hopkins Rd, Laurel, MD 20723

CYNTHIA S. FRONING, JAMES C. GREEN, AND STEVEN N. OSTERMAN
Center for Astrophysics and Space Astronomy, 389 UCB, University of Colorado, Boulder, CO 80309

Draft version February 17, 2010

ABSTRACT

We present recent observations from the *HST*-Cosmic Origins Spectrograph aimed at characterizing the auroral emission from the extrasolar planet HD209458b. We obtained medium-resolution ($R \sim 20{,}000$) far-ultraviolet (1150 – 1700 Å) spectra at both the Phase 0.25 and Phase 0.75 quadrature positions as well as a stellar baseline measurement at secondary eclipse. This analysis includes a catalog of stellar emission lines and a star-subtracted spectrum of the planet. We present an emission model for planetary H_2 emission, and compare this model to the planetary spectrum. No unambiguously identifiable atomic or molecular features are detected, and upper limits are presented for auroral/dayglow line strengths. An orbital velocity cross-correlation analysis finds a statistically significant ($3.8\ \sigma$) feature at $+15$ ($\pm$ 20) km s^{-1} in the rest frame of the planet, at λ1582 Å. This feature is consistent with emission from H_2 $B - X$ $(2 - 9)$ P(4) (λ_{rest} = 1581.11 Å), however the physical mechanism required to excite this transition is unclear. We compare limits on relative line strengths seen in the exoplanet spectrum with models of ultraviolet fluorescence to constrain the atmospheric column density of neutral hydrogen between the star and the planetary surface. These results support models of short period extrasolar giant planets with weak magnetic fields and extended atomic atmospheres.

Subject headings: stars: planetary systems — stars: individual (HD209458) — stars: atmospheres — ultraviolet: stars

No clear detection of magnetic field. The interpretation in this paper is strongly optimistic

Bibliography

- Fehrenbach, Dawidowicz, Marion, Aurores boréales et australes. GNGL Productions, 2001.
- Lilensten, Bornarel. Sous les feux du soleil. Grenoble sciences, EDP sciences, 2002.
- Le système solaire revisité sous la direction de Jean Lilensten. Eyrolles 2006.
- Du Soleil à la Terre. Lilensten et Blelly. PUG 1999
- Kivelson Russel. Introduction to space plasma. Cambridge 1995